Science
AAAS

Title: Engram Cells Retain Memory Under Retrograde Amnesia

Authors: Tomás J. Ryan[1,2,*], Dheeraj S. Roy[1,*], Michele Pignatelli[1,*], Autumn Arons[1,2], and Susumu Tonegawa[1,2,†]

Affiliations:

[1] RIKEN-MIT Center for Neural Circuit Genetics at the Picower Institute for Learning and Memory, Department of Biology and Department of Brain and Cognitive Sciences, Massachusetts Institute of Technology, Cambridge, MA 02139, USA

[2]Howard Hughes Medical Institute, Massachusetts Institute of Technology, Cambridge, MA 02139, USA

† Correspondence to: tonegawa@mit.edu

* These authors contributed equally to this work.

Abstract: Memory consolidation is the process by which a newly formed and unstable memory transforms into a stable long-term memory. It is unknown whether the process of memory consolidation occurs exclusively by the stabilization of memory engrams. By employing learning-dependent cell labeling, we identified an increase of synaptic strength and dendritic spine density specifically in consolidated memory engram cells. While these properties are lacking in the engram cells under protein synthesis inhibitor-induced amnesia, direct optogenetic activation of these cells results in memory retrieval, and this correlates with the retained engram cell-specific connectivity. We propose that a specific pattern of connectivity of engram cells may be crucial for memory information storage and that strengthened synapses in these cells critically contribute to the memory retrieval process.

One Sentence Summary: Memory can be retrieved by optogenetic activation of engram cells in retrograde amnesia.

Main Text:

Memory consolidation is the phenomenon whereby a newly formed memory transitions from a fragile state to a stable, long-term state (*1-3*). The defining feature of consolidation is a finite time window that begins immediately after learning, during which a memory is susceptible to disruption such as protein synthesis inhibition (*4-6*), resulting in retrograde amnesia. The stabilization of synaptic potentiation is the dominant cellular model of memory consolidation (*7-10*) because protein synthesis inhibitors disrupt late-phase long-term potentiation of *in vitro* slice preparations (*11-13*). Although much is known about the cellular mechanisms of memory consolidation it remains unknown whether these processes occur in memory engram cells. It may be possible to characterize cellular consolidation and empirically separate mnemonic properties in retrograde amnesia by directly probing and manipulating memory engram cells in the brain. The term memory engram originally referred to the hypothetical learned information stored in the brain, which must be reactivated for recall (*14-15*). Recently, several groups demonstrated that specific hippocampal cells that are activated during memory encoding are both sufficient (*16-18*) and necessary (*19-20*) for driving future recall of a contextual fear memory, and thus represent a component of a distributed memory engram (*21*). Here, we applied this engram technology to the issue of cellular consolidation and retrograde amnesia.

We employed the previously established method for tagging the hippocampal dentate gyrus (DG) component of a contextual memory engram with mCherry (see Materials and Methods, fig. S1, and (*16, 22*)). To disrupt consolidation we systemically injected the protein synthesis inhibitor anisomycin (ANI) or saline (SAL) as a control immediately after contextual fear conditioning (CFC) (Fig. 1A). The presynaptic neurons of the entorhinal cortex (EC) were constitutively labeled with ChR2 expressed from an AAV_8-CaMKIIα-ChR2-EYFP virus (Fig. 1B). Voltage clamp recordings of paired engram ($mCherry^+$) and non-engram ($mCherry^-$) DG cells were conducted simultaneously with optogenetic stimulation of $ChR2^+$ perforant path (PP) axons (Fig. 1C, D). $mCherry^+$ cells of the SAL group showed significantly greater synaptic strength than $mCherry^+$ cells of the ANI engram group, but the $mCherry^-$ cells of the SAL and ANI groups were of comparable synaptic strength (Fig. 1E). Calculation of AMPA/NMDA current ratios (*23*) showed that at 24 hours post-training, $mCherry^+$ engram cells displayed potentiated synapses relative to paired $mCherry^-$ non-engram cells in the SAL group (Fig. 1E). However, no such difference between $mCherry^+$ and $mCherry^-$ was observed in the ANI group.

In addition, mCherry$^+$ engram cells of the SAL group showed significantly greater AMPA/NMDA current ratios than mCherry$^+$ engram cells of the ANI group. Analysis of miniature EPSCs of engram and non-engram cells of both SAL and ANI groups showed the same pattern (fig. S2).

We also quantified dendritic spine density for DG engram cells labeled with an AAV_9-TRE-ChR2-EYFP virus. Spine density of ChR2$^+$ cells was significantly higher than corresponding ChR2$^-$ cells in the SAL group (Fig. 1F. fig. S3), but spine densities of ChR2$^+$ and ChR2$^-$ cells of the ANI group were similar (see Materials and Methods). Spine density of ChR2$^+$ cells of the SAL group was significantly higher than that of ANI ChR2$^+$ cells (Fig.1F), but ChR2$^-$ cells were comparable. This result was confirmed by analysis of the membrane capacitance (fig. S4G). ChR2 expression did not affect intrinsic properties of DG cells *in vitro* (fig. S5A-E). Direct bath application of ANI did not affect intrinsic cellular properties *in vitro* (fig. S5F), although it mildly reduced synaptic currents acutely (fig. S5G-I). Importantly, when anisomycin was injected into c-fos-tTA animals 24 hours post-CFC and engram labeling, engram-cell specific increases in dendritc spine density and synaptic strength were undisturbed (fig. S6). We also examined engram cells labeled by a context-only experience (*17*), and found equivalent engram-cell increases in spine density and synaptic strength (fig. S7) as those labeled by CFC.

DG cells receive information from EC and relay it to area CA3 via the mossy fibers. We labeled DG engram cells using an AAV_9-TRE-ChR2-EYFP virus and simultaneously labeled CA3 engram cells using an AAV_9-TRE-mCherry virus (Fig. 1G). Connection probability was assessed 24 hours post-CFC by stimulating DG ChR2$^+$ cell terminals optogenetically and recording excitatory postsynaptic potentials in CA3 mCherry$^+$ and mCherry$^-$ cells in *ex vivo* preparations. CA3 mCherry$^+$ engram cells showed a significantly higher probability of connection than mCherry$^-$ cells with DG ChR2$^+$ engram cells, demonstrating preferential engram cell to engram cell connectivity. Importantly, this form of engram pathway-specific connectivity was unaffected by post-training administration of ANI (Fig. 1G).

We next tested the behavioral effect of optogenetically stimulating engram cells in amnesic mice (Fig 2A). During CFC training in Context B, both SAL and ANI groups responded to the unconditioned stimuli at equivalent levels (fig. S8). One day post-training, the SAL group displayed robust freezing behavior to the conditioned stimulus of context B, whereas the ANI

group showed substantially less freezing behavior (Fig. 2C). Two days post-training, mice were placed into the distinct context A for a 12 min test session consisting of four 3 min epochs of blue light on or off. During this test session, neither group showed freezing behavior during Light-Off epochs, but both froze significantly during Light-On epochs (Fig. 2D). Remarkably, no difference in the levels of light-induced freezing behavior was observed between groups. Three days post-training, the mice were again tested in context B to assay the conditioned response, and retrograde amnesia for the conditioning context was still clearly evident (Fig. 2E). Subjects treated with SAL or ANI following the labeling of a neutral contextual engram (i.e. no shock) did not show freezing behavior in response to light stimulation of engram cells (Fig. 2D). We replicated the DG retrograde amnesia experiment using an alternative widely-used protein synthesis inhibitor, cycloheximide (CHM) (fig. S9). We examined whether ANI administration immediately after CFC altered the activity dependent synthesis of ChR2-EYFP in DG cells and found that this was not the case (Fig. 2F-H). Nevertheless, the dosage of anisomycin used in this study did inhibit protein synthesis in the DG as shown by Arc^{+} cell counting (fig. S10). Thus, the dosage of ANI used was sufficient to induce amnesia, but was insufficient to impair c-fos-tTA driven synthesis of virally delivered ChR2-EYFP in DG cells. Extracellular recordings from SAL and ANI-treated mice confirmed the cell counting results (Fig. 2I-K). In line with fig. S6 and previous reports (*24*), anisomycin injection 24 hours post-CFC did not cause retrograde amnesia (fig. S11). To provide a negative control for light-induced memory retrieval in amnesia, we disrupted memory encoding by activating hM4Di DREADDs receptors (*25*) downstream of the DG, in hippocampal CA1, during CFC, and found that subsequent DG engram activation did not elicit memory retrieval (fig. S12).

The recovery from amnesia by direct light activation of ANI-treated DG engram cells was unexpected because these cells showed neither synaptic potentiation nor increased dendritic spine density. We conducted additional behavioral experiments to confirm and characterize the phenomenon. First, we investigated whether recovery from amnesia can be demonstrated by light-induced optogenetic place avoidance test (OptoPA); this would be a measure of an active fear memory recall (see Materials and Methods and (*18*)), rather than a passive fear response monitored by freezing. SAL and ANI groups displayed equivalent levels of avoidance of the target zone in response to light activation of the DG engram (Fig. 3A). Second, in our previous study we showed that an application of the standard protocol (i.e. 20 Hz) for activation of the

CA1 engram was not effective for memory recall (*17*). However, we found that a 4 Hz protocol applied to the CA1 engram of the SAL and ANI groups elicited similar recovery from amnesia (Fig. 3B). Third, we employed tone fear conditioning (TFC) and manipulated the fear engram in lateral amygdala (LA) (*26*) and found light-induced recovery of memory from amnesia. Fourth, we asked whether amnesia caused by disruption of reconsolidation of a contextual fear memory (*27-28*) can also be recovered by light-activation of DG engram cells, and indeed it was found to be the case (Fig. 3D). We applied the memory inception method (Materials and Methods, (*17, 29*) to DG engram cells and found that both SAL and ANI groups showed freezing behavior that was specific to the original Context A, demonstrating that light-activated Context A engrams formed in the presence of ANI can function as a CS in a context-specific manner (Fig. 3E). Lastly, we tested the longevity of CFC amnesic engrams for memory recovery by light activation, and found that indeed memory recall could be observed 8 days post-training (fig. S13).

Interactions between the hippocampus and amygdala are crucial for contextual fear memory encoding and retrieval (18). c-Fos expression increases in the hippocampus and amygdala upon exposure of an animal to conditioned stimuli (*30-31*). These previous observations open up the possibility of obtaining cellular level evidence supporting the behavioral level finding that the recovery from amnesia can be accomplished by direct light activation of ANI-treated DG engram cells. Thus, we compared the effects of natural recall and light-induced recall on amygdala c-Fos$^+$ cell counts in amnesic mice (Fig. 4A-C). c-Fos$^+$ cell counts (Fig. 4B) were significantly lower in basolateral amygdala (BLA) and central amygdala (CeA) of ANI-treated mice compared to SAL mice when natural recall cues were delivered, showing that amygdala activity correlates with fear memory expression (Fig. 4C). In contrast, light-induced activation of the contextual engram cells resulted in equivalent amygdala c-Fos$^+$ counts in SAL and ANI groups (Fig. 4C), supporting the optogenetic behavioral data.

Next, we modified this protocol to include labeling of CA3 and BLA engram cells with mCherry and examined the effects of light-induced activation of DG engram cells on the overlap of mCherry$^+$ engram cells and c-Fos$^+$ recall-activated cells in CA3 and BLA (Fig. 4D). The purpose of this experiment was to investigate whether there is preferential connectivity between the upstream engram cells in DG and the downstream engram cells in CA3 or BLA. Natural recall cues resulted in above chance c-Fos$^+$/mCherry$^+$ overlap in both CA3 and BLA, supporting

the physiological connectivity data (Fig. 4E-K). c-Fos$^+$/mCherry$^+$ overlap was significantly reduced in the ANI group compared to the SAL group, but was still higher than chance levels, presumably reflecting incomplete amnesic effects of anisomycin (Fig. 4K). Importantly, light-activation of DG engram cells resulted in equivalent c-Fos$^+$/mCherry overlap as natural cue-induced recall, and this was unaffected by post-CFC anisomycin treatment. These data suggest that there is preferential and protein synthesis-independent functional connectivity between DG and CA3 engram cells, supporting the physiological data (Fig. 1G), and that this connectivity also applies between DG and BLA engram cells.

We previously showed that DG cells activated during CFC training and labeled with ChR2 via the promoter of an immediate early gene (IEG) can evoke a freezing response when they are reactivated optogenetically one to two days later (*16*), and this has since been achieved in the cortex (*21*). We have also shown that these DG cells, if light-activated while receiving a US, can serve as a surrogate context-specific CS to create a false CS-US association (*17-18*), and that activation of DG or amygdala engram cells can induce place preference (*18*). Furthermore, recent studies showed that optogenetic inhibition of these cells in DG, CA3, or CA1 impairs expression of a CFC memory (*19-20*). Together, these findings show that engram cells activated by CFC training are both sufficient and necessary to evoke memory recall, satisfying two crucial attributes in defining a component of a contextual fear memory engram (*15*). What has been left to be demonstrated, however, is that these DG cells undergo enduring physical changes as an experience is encoded and its memory is consolidated. Although synaptic potentiation has long been suspected as a fundamental mechanism for memory and as a crucial component of the enduring physical changes induced by experience, this has not been directly demonstrated, until the current study, as a property of the engram cells. Our data have directly linked the optogenetically and behaviorally defined memory engram cells to synaptic plasticity.

Based on a large volume of previous studies, (*1-3, 7-8, 32-34*), a concept has emerged where retrograde amnesia arises from consolidation failure as a result of disrupting the process that converts a fragile memory engram, formed during the encoding phase, into a stable engram with persistently augmented synaptic strength and spine density. Indeed, our current study has demonstrated that amnesic engram cells in the DG one day after CFC training display low levels of synaptic strength and spine density that are indistinguishable from non-engram cells of the same DG. This correlated with a lack of memory recall elicited by contextual cues. Intriguingly,

however, direct activation of DG engram cells of the ANI group elicited as much freezing behavior as the activation of these cells of the SAL group. This unexpected finding is supported by a set of additional cellular and behavioral experiments. While amygdala engram cell reactivation upon exposure to the conditioned context is significantly lower in the ANI group compared to the SAL group, optogenetic activation of DG engram cells results in normal reactivation of downstream CA3 and BLA engram cells (Fig. 4). At the behavioral level, the amnesia rescue was observed under a variety of different conditions in which one or more parameters were altered (Fig. 2-3, fig. S9, and fig. S13). Thus, our overall findings indicate that memory engrams survive a post-training administration of protein synthesis inhibitors during the consolidation window and that the memory remains retrievable by ChR2-mediated direct engram activation even after retrograde amnesia is induced. The drive initiated with light-activation of one component of a distributed memory engram (like that in the DG) is sufficient to reactivate engrams in downstream regions (like that in CA3 and BLA) that would also be affected by the systemic injection of a protein synthesis inhibitor (ANI).

Our findings suggest that while a rapid increase of synaptic strength is likely to be crucial during the encoding phase, the augmented synaptic strength is not a crucial component of the stored memory (*35*-*37*). This notion is consistent with a recent study showing that an artificial memory could be reversibly disrupted by depression of synaptic strength (*38*). On the other hand, persistent and specific connectivity of engram cells which we find between DG engram cells and downstream CA3 or BLA engram cells in both SAL and ANI groups may represent a fundamental mechanism of memory information storage (*39*). These findings also suggest that the primary role of augmented synaptic strength during and after the consolidation phase may be to provide natural recall cues with efficient access to the soma of engram cells for their reactivation and, hence, recall.

The integrative memory engram-based approach employed here for parsing memory and amnesia into encoding, consolidation, and retrieval aspects may be of wider use to other experimental and clinical cases of amnesia, such as Alzheimer's disease (*40*).

Acknowledgments: We thank X. Liu and B. Roth for sharing reagents; X. Zhou, Y. Wang, W. Yu, S. Huang, and T. O'Connor for technical assistance; J. Z. Young for proofreading; and other members of the Tonegawa Lab for their comments and support. This work was supported by the RIKEN Brain Science Institute, Howard Hughes Medical Institute, and the JPB Foundation (to S.T.).

Figures

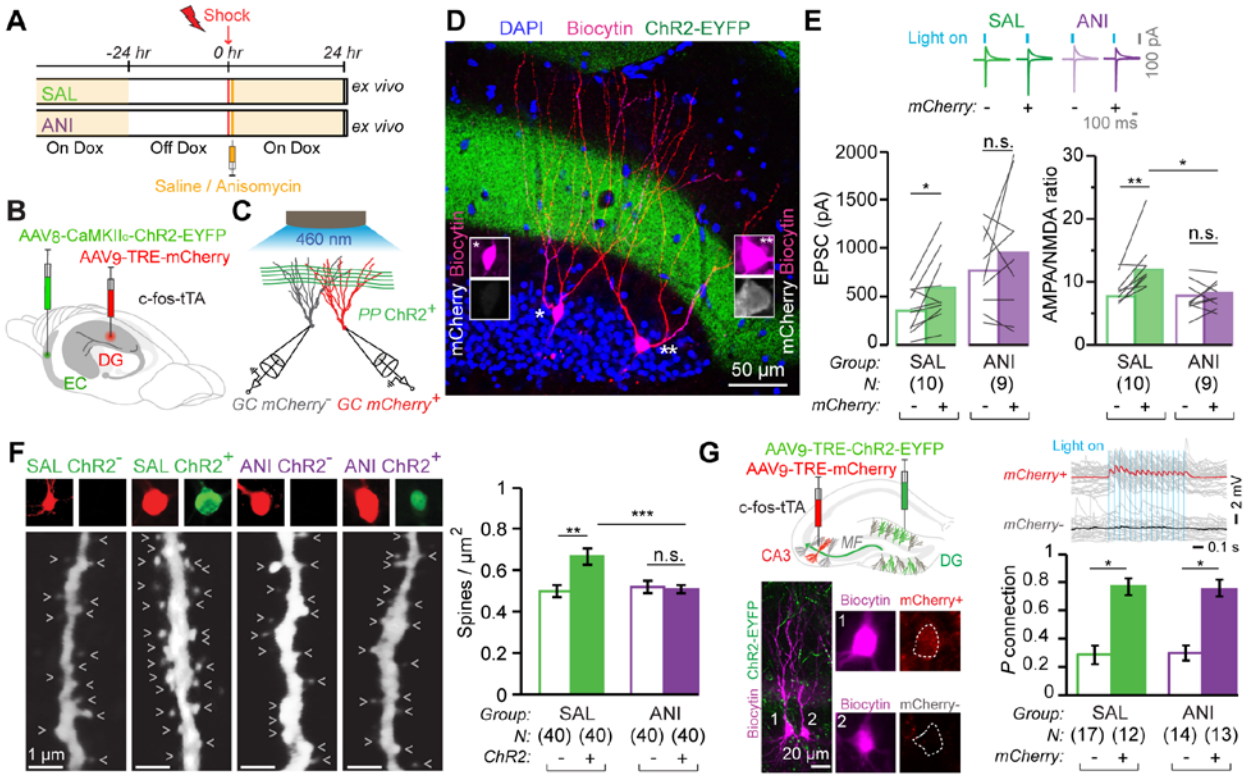

Figure 1: Synaptic Plasticity and Connectivity of Engram Cells.

(A) Mice taken Off DOX 24 hrs before contextual fear conditioning (CFC) and dispatched 24 hrs post training. Saline (SAL) or anisomycin (ANI) administered immediately after training.

(B) AAV_8-CaMKIIα-ChR2-EYFP and AAV_9-TRE-mCherry viruses injected into the entorhinal cortex and dentate gyrus, respectively, of c-fos-tTA mice.

(C) Paired recordings of engram (red) and non-engram (grey) DG cells during optogenetic stimulation of $ChR2^+$ perforant path (PP) axons.

(D) Representative image of a pair of recorded biocytin-labeled engram ($mCherry^+$) and non-engram ($mCherry^-$) DG cells. Note $ChR2^+$ PP axons in green.

(E) (Top) Example traces of AMPA and NMDA receptor-dependent postsynaptic currents in $mCherry^+$ and $mCherry^-$ cells, evoked by light activation of $ChR2^+$ PP axons. (Bottom) EPSC

amplitudes and AMPA/NMDA current ratios of $mCherry^+$ and $mCherry^-$ cells of the two groups are displayed as means (columns) and individual paired data points (grey lines). Paired t-test * $p < 0.05$, ** $p < 0.001$. SAL group compared with the ANI group, unpaired t-test * $p < 0.05$.

(F) (Left) Representative confocal images of biocytin filled dendritic fragments derived from SAL and ANI groups for $ChR2^+$ and $ChR2^-$ cells (arrow heads: dendritic spines). (Right) Average dendritic spine density showing an increase occurring exclusively in $ChR2^+$ fragments. Data are represented as mean ± SEM. Unpaired t tests ** $p < 0.01$, *** $p < 0.001$.

(G) Engram Connectivity. (Top left) AAV_9-TRE-ChR2-EYFP and AAV_9-TRE-mCherry viruses, injected into the DG and CA3, respectively, of c-fos-tTA mice. (Bottom left) Example of $mCherry^+$ (1) and $mCherry^-$ (2) biocytin-filled CA3 pyramidal cells. Note $ChR2^+$ mossy fibers (MF) in green. (Top Right) $mCherry^+$ cell but not $mCherry^-$ cell displayed EPSPs in response to optogenetic stimulation of MF. (Bottom Right) Probability of connection of DG $ChR2^+$ engram axons and CA3 $mCherry^+$ and $mCherry^-$ cells. Error bars are approximated by binomial distribution. Fisher's exact test: * $p < 0.05$.

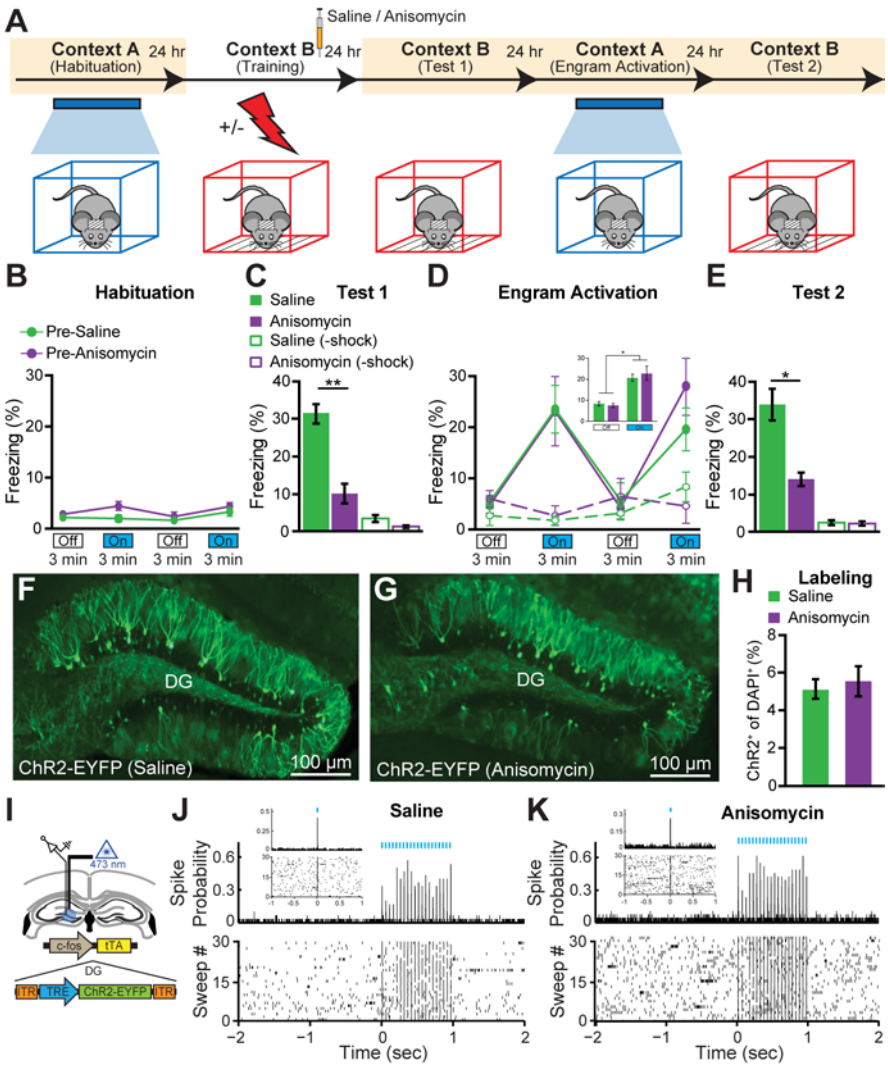

Figure 2: Optogenetic Stimulation of DG Engram Cells Restores Fear Memory in Retrograde Amnesia.

(A) Behavioral schedule. Beige shading signifies that subjects are On DOX, precluding ChR2 expression. Mice taken off DOX 24-30 hrs before CFC in Context B. SAL or ANI was injected into the mice after training.

(B) Habituation to Context A with Light-Off and Light-On epochs. Blue light stimulation of the DG did not cause freezing behavior in naïve, unlabelled mice of the pre-SAL (n = 10) or pre-ANI (n = 8) groups.

(C) Memory recall in Context B 1 day post-training (Test 1). ANI group displayed significantly less freezing than SAL group ($p < 0.005$). No-shock groups with SAL ($n = 4$) or ANI ($n = 4$) did not display freezing upon re-exposure to Context B.

(D) Memory recall in Context A 2 days post-training (Engram Activation) with Light-Off and Light-On epochs. Freezing for the two Light-Off and Light-On epochs are further averaged in the inset. Significant freezing due to light stimulation was observed in both the SAL ($p < 0.01$) and ANI groups ($p < 0.05$). Freezing levels did not differ between groups. SAL and ANI-treated no-shock control groups did not freeze in response to light stimulation of context B engram cells.

(E) Memory recall in Context B 3 days post-training (Test 2). ANI group displayed significantly less freezing than SAL group ($p < 0.05$).

(F, G) Images showing DG sections from c-fos-tTA mice 24 hrs after SAL or ANI treatment.

(H) ChR2-EYFP cell counts from DG sections of SAL ($n = 3$) and ANI ($n = 4$) groups.

(I) *In vivo* anesthetized recordings (see Materials and Methods).

(J, K) Light pulses induced spikes in DG neurons recorded from head-fixed anesthetized c-fos-tTA mice 24 hrs after treatment with either SAL or ANI.

Data presented as mean ± SEM.

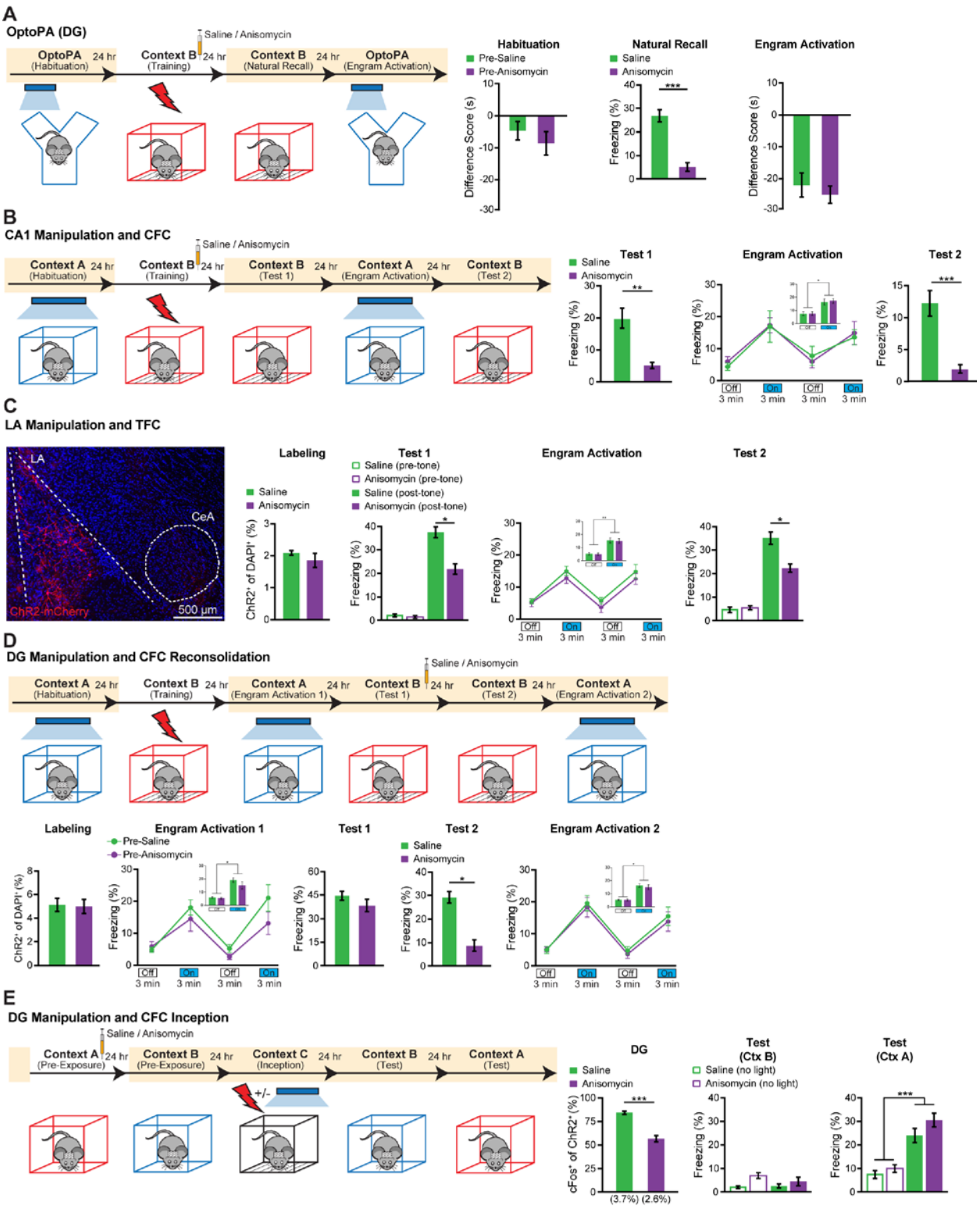
A
OptoPA (DG)
Saline / Anisomycin
OptoPA (Habituation) 24 hr
Context B (Training) 24 hr
Context B (Natural Recall) 24 hr
OptoPA (Engram Activation)
Habituation
Pre-Saline
Pre-Anisomycin
Difference Score (s)
Natural Recall
Saline
Anisomycin
Freezing (%)
***
Engram Activation
Difference Score (s)
B
CA1 Manipulation and CFC
Saline / Anisomycin
Context A (Habituation) 24 hr
Context B (Training) 24 hr
Context B (Test 1) 24 hr
Context A (Engram Activation) 24 hr
Context B (Test 2)
Test 1
Saline
Anisomycin
**
Freezing (%)
Engram Activation
Off
On
3 min
Test 2
***
C
LA Manipulation and TFC
LA
CeA
ChR2-mCherry
500 µm
Labeling
Saline
Anisomycin
ChR2+ of DAPI+ (%)
Test 1
Saline (pre-tone)
Anisomycin (pre-tone)
Saline (post-tone)
Anisomycin (post-tone)
*
Freezing (%)
Engram Activation
Test 2
D
DG Manipulation and CFC Reconsolidation
Saline / Anisomycin
Context A (Habituation) 24 hr
Context B (Training) 24 hr
Context A (Engram Activation 1) 24 hr
Context B (Test 1) 24 hr
Context B (Test 2) 24 hr
Context A (Engram Activation 2)
Labeling
Engram Activation 1
Pre-Saline
Pre-Anisomycin
Test 1
Test 2
Saline
Anisomycin
Engram Activation 2
E
DG Manipulation and CFC Inception
Saline / Anisomycin
Context A (Pre-Exposure) 24 hr
Context B (Pre-Exposure) 24 hr
Context C (Inception) 24 hr
Context B (Test) 24 hr
Context A (Test)
+/-
DG
Saline
Anisomycin
cFos+ of ChR2+ (%)
(3.7%) (2.6%)
Test (Ctx B)
Saline (no light)
Anisomycin (no light)
Test (Ctx A)

Figure 3: Recovery of Memory from Amnesia under a Variety of Conditions.

(A) DG engram activation and optogenetic place avoidance (OptoPA). During habituation neither group displayed significant avoidance of target zone. For Natural Recall the ANI group ($n = 10$) displayed significantly less freezing than SAL group ($n = 12$) in Context B ($p < 0.005$). SAL and ANI displayed similar levels of OptoPA.

(B) CA1 engram activation and CFC. 1 day post-CFC (Test 1) ANI group ($n = 9$) displayed significantly less freezing than SAL group ($n = 10$) in Context B ($p < 0.01$). 2 days post-training (Engram Activation), light-activation of CA1 engrams elicited freezing in both SAL ($p < 0.01$) and ANI groups ($p < 0.001$). 3 days post-training (Test 2) ANI group froze less than SAL group in Context B ($p < 0.01$).

(C) Lateral amygdala (LA) engram activation and tone fear conditioning (TFC). The behavioral schedule was identical to that in Fig. 3B, except that context tests were replaced with tone tests in Context C (Materials and Methods). (Left) example image of ChR2-mCherry labeling of LA neurons. 2% of DAPI cells were labeled by ChR2. (Right) 1 day post-training (Test 1), ANI group ($n = 9$) displayed significantly less freezing to tone than SAL group ($n = 9$) ($p < 0.05$). 2 days post-training (Engram Activation), significant light-induced freezing was observed for both SAL ($p < 0.005$) and ANI groups ($p < 0.005$). 3 days post-training (Test 2) ANI group froze less to tone than SAL group ($p < 0.05$).

(D) DG engram activation and CFC reconsolidation. ANI ($n = 11$) and SAL ($n = 11$) groups showed similar levels of ChR2 labeling. Both groups showed light-induced freezing behavior 1 day post-training (Engram Activation 1), pre-SAL ($P < 0.001$), pre-ANI ($P < 0.02$). 2 days post training, (Test 1) the fear memory was reactivated by exposure to Context B, and SAL or ANI injected. 3 days post-training, (Test 2) the ANI group froze significantly less than SAL to Context B ($p < 0.01$). 4 days post-training, (Engram Activation 2) significant light-induced freezing was observed for the SAL ($p < 0.001$) and ANI ($p < 0.003$) groups.

(E) DG Inception (Materials and Methods) following contextual memory amnesia. Context-only engram was labeled for target Context A, followed by injection of SAL ($n = 11$) or ANI ($n = 11$).

Amnesia demonstrated in ANI group by decreased $ChR2^{+}/c\text{-}Fos^{+}$ co-labeling following Context A re-exposure 1 day post labeling.

Following fear inception, neither SAL nor ANI groups displayed freezing behavior in Context B, while both groups displayed significant freezing in Context A, with no significant difference between groups. No-light inception SAL (n = 7) and ANI (n = 6) controls displayed no freezing to Context A or B. Statistical comparison are performed by using unpaired t tests, *** $p < 0.001$.

Data presented as mean ± SEM.

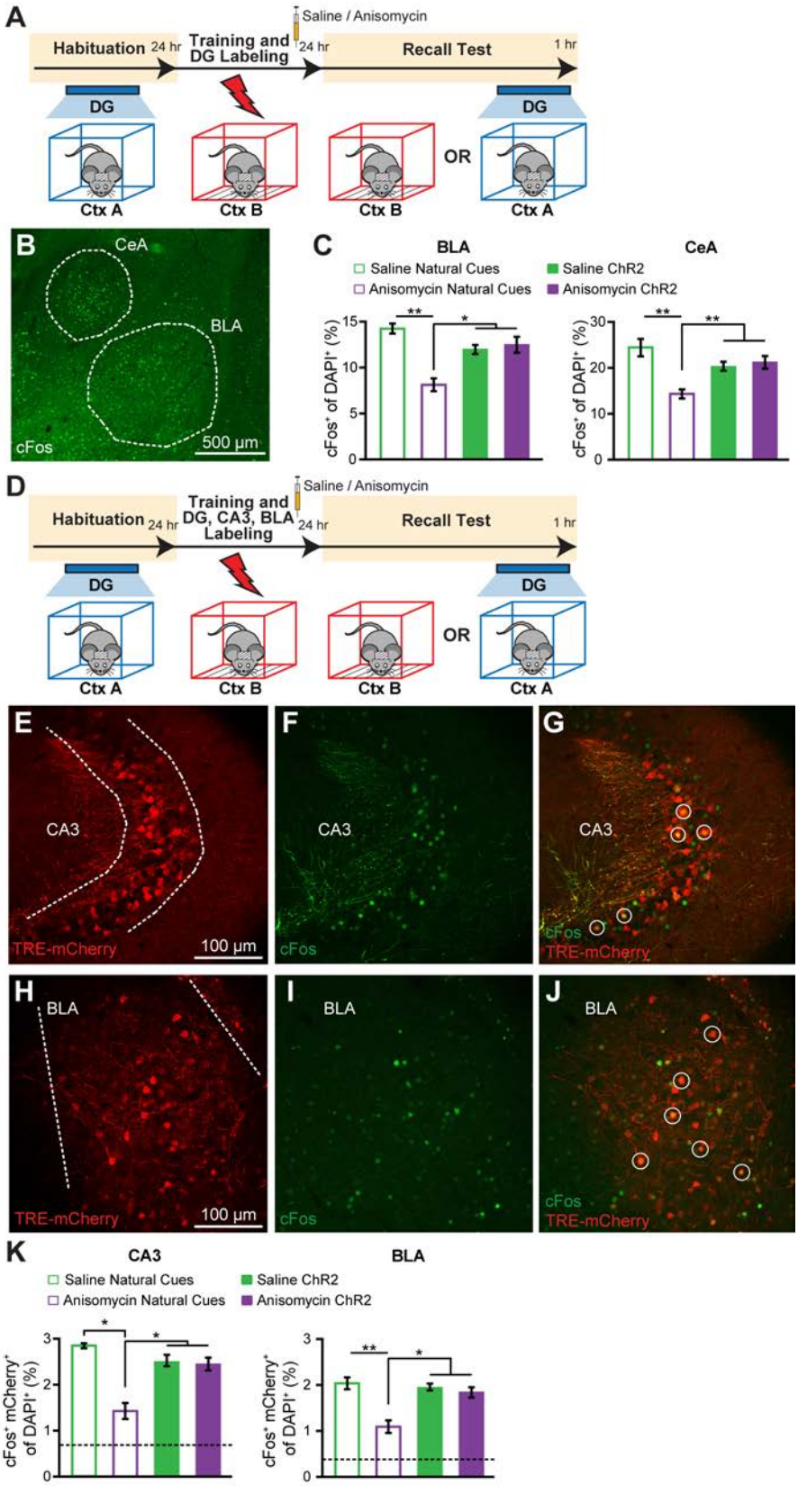
A
Saline / Anisomycin
Habituation 24 hr
Training and DG Labeling
24 hr
Recall Test
1 hr
DG
DG
OR
Ctx A
Ctx B
Ctx B
Ctx A
B
CeA
BLA
cFos
500 µm
C
BLA
CeA
Saline Natural Cues
Saline ChR2
Anisomycin Natural Cues
Anisomycin ChR2
cFos+ of DAPI+ (%)
D
Saline / Anisomycin
Habituation 24 hr
Training and DG, CA3, BLA Labeling
24 hr
Recall Test
1 hr
DG
DG
OR
Ctx A
Ctx B
Ctx B
Ctx A
E
CA3
TRE-mCherry
100 µm
F
CA3
cFos
G
CA3
cFos
TRE-mCherry
H
BLA
TRE-mCherry
100 µm
I
BLA
cFos
J
BLA
cFos
TRE-mCherry
K
CA3
BLA
Saline Natural Cues
Saline ChR2
Anisomycin Natural Cues
Anisomycin ChR2
cFos+ mCherry+ of DAPI+ (%)

Figure 4: Amygdala Activation and Functional Connectivity in Amnesia by Light Activation of DG Engram

(A) Schedule for cell counting experiments. Mice were either given a natural recall session in Context B, or a light-induced recall session in Context A. Mice were perfused 1 hr post recall.

(B) Representative image showing c-Fos expression in the basolateral amygdala (BLA) and central amygdala (CeA).(C) c-Fos$^+$ cell counts in the BLA and CeA of mice following natural or light-induced recall (n = 3-4 per group).

(D) Schedule for cell counting experiments. c-fos-tTA mice with AAV_9-TRE-ChR2-EYFP injected into the DG and AAV_9-TRE-mCherry injected into both CA3 and BLA were fear conditioned off DOX, and 1 day later were given a natural recall session in Context B, or a light-induced recall session in Context A. Mice were perfused 1 hr post recall.

(E – G) Representative images showing mCherry engram cell labeling, c-Fos expression, mCherry$^+$/c-Fos$^+$ overlap in CA3.

(H – J) Representative images showing mCherry engram cell labeling, c-Fos expression, mCherry/c-Fos overlap in BLA.

(K) c-Fos$^+$/mCherry$^+$ overlap cell counts in CA3 and BLA of mice following natural or light-induced recall (n = 3 - 4 per group). Chance levels were estimated at 0.76 (CA3) and 0.42 (BLA). Data are presented as mean ± SEM. Statistical comparison are performed by using unpaired t tests, * $p < 0.05$, ** $p < 0.01$.

References:

1. G. E. Müller, A. Pilzecker, *Z. Psychol* **SI:**, 1 (1900).
2. C. P. Duncan, *J Comp Physiol Psychol* **42**, 32 (Feb, 1949).
3. J. L. McGaugh, *Science* **287**, 248 (Jan 14, 2000).
4. J. B. Flexner, L. B. Flexner, E. Stellar, *Science* **141**, 57 (Jul 5, 1963).
5. L. B. Flexner, J. B. Flexner, R. B. Roberts, *Science* **155**, 1377 (Mar 17, 1967).
6. H. P. Davis, L. R. Squire, *Psychol Bull* **96**, 518 (Nov, 1984).
7. E. R. Kandel, *Science* **294**, 1030 (Nov 2, 2001).
8. R. J. Kelleher, 3rd, A. Govindarajan, S. Tonegawa, *Neuron* **44**, 59 (Sep 30, 2004).
9. T. Takeuchi, A. J. Duszkiewicz, R. G. Morris, *Philos Trans R Soc Lond B Biol Sci* **369**, 20130288 (Jan 5, 2014).
10. A. Govindarajan, I. Israely, S. Y. Huang, S. Tonegawa, *Neuron* **69**, 132 (Jan 13, 2011).
11. M. Krug, B. Lossner, T. Ott, *Brain Res Bull* **13**, 39 (Jul, 1984).
12. U. Frey, M. Krug, K. G. Reymann, H. Matthies, *Brain Res* **452**, 57 (Jun 14, 1988).
13. Y. Y. Huang, P. V. Nguyen, T. Abel, E. R. Kandel, *Learn Mem* **3**, 74 (Sep-Oct, 1996).
14. R. Semon, *Die Mneme als erhaltendes Prinzip im Wechsel des organischen Geschehens*. (Wilhelm Engelmann, Leipzig, 1904).
15. S. A. Josselyn, *J Psychiatry Neurosci* **35**, 221 (Jul, 2010).
16. X. Liu *et al.*, *Nature* **484**, 381 (Apr 19, 2012).
17. S. Ramirez *et al.*, *Science* **341**, 387 (Jul 26, 2013).
18. R. L. Redondo *et al.*, *Nature* **513**, 426 (Sep 18, 2014).
19. C. A. Denny *et al.*, *Neuron* **83**, 189 (Jul 2, 2014).
20. K. Z. Tanaka *et al.*, *Neuron*, (Oct 8, 2014).
21. K. K. Cowansage *et al.*, *Neuron*, (Oct 8, 2014).
22. L. G. Reijmers, B. L. Perkins, N. Matsuo, M. Mayford, *Science* **317**, 1230 (Aug 31, 2007).
23. R. L. Clem, R. L. Huganir, *Science* **330**, 1108 (Nov 19, 2010).
24. A. Suzuki *et al.*, *J Neurosci* **24**, 4787 (May 19, 2004).
25. B. N. Armbruster, X. Li, M. H. Pausch, S. Herlitze, B. L. Roth, *Proc Natl Acad Sci U S A* **104**, 5163 (Mar 20, 2007).
26. J. H. Han *et al.*, *Science* **323**, 1492 (Mar 13, 2009).
27. J. R. Misanin, R. R. Miller, D. J. Lewis, *Science* **160**, 554 (May 3, 1968).
28. K. Nader, G. E. Schafe, J. E. Le Doux, *Nature* **406**, 722 (Aug 17, 2000).
29. X. Liu, S. Ramirez, S. Tonegawa, *Philos Trans R Soc Lond B Biol Sci* **369**, 20130142 (2014).
30. A. Besnard, S. Laroche, J. Caboche, *Brain Struct Funct* **219**, 415 (Jan, 2014).
31. J. Hall, K. L. Thomas, B. J. Everitt, *Eur J Neurosci* **13**, 1453 (Apr, 2001).
32. J. L. McGaugh, *Science* **153**, 1351 (Sep 16, 1966).
33. Y. Dudai, *Annu Rev Psychol* **55**, 51 (2004).
34. J. P. Johansen, C. K. Cain, L. E. Ostroff, J. E. LeDoux, *Cell* **147**, 509 (Oct 28, 2011).
35. R. R. Miller, L. D. Matzel, *Learn Mem* **13**, 491 (Sep-Oct, 2006).
36. C. A. Miller, J. D. Sweatt, *Learn Mem* **13**, 498 (Sep-Oct, 2006).
37. S. Chen *et al.*, *Elife* **3**, (Nov 17, 2014).
38. S. Nabavi *et al.*, *Nature* **511**, 348 (Jul 17, 2014).
39. D. O. Hebb, *The organization of behavior; a neuropsychological theory*. (Wiley, New York, 1949).
40. S. Daumas *et al.*, *Learn Mem* **15**, 625 (Sep, 2008).

Title: Engram Cells Retain Memory Under Retrograde Amnesia

Authors: Tomás J. Ryan[1,2,*], Dheeraj S. Roy[1,*], Michele Pignatelli[1,*], Autumn Arons[1,2], and Susumu Tonegawa[1,2,†]

Affiliations:

[1] RIKEN-MIT Center for Neural Circuit Genetics at the Picower Institute for Learning and Memory, Department of Biology and Department of Brain and Cognitive Sciences, Massachusetts Institute of Technology, Cambridge, MA 02139, USA

[2] Howard Hughes Medical Institute, Massachusetts Institute of Technology, Cambridge, MA 02139, USA

† Correspondence to: tonegawa@mit.edu

* These authors contributed equally to this work.

Supplementary Materials:

Materials and Methods

Figures S1-S13

References

Materials and Methods

Subjects

All experiments were conducted in accordance with U.S. National Institutes of Health guidelines and the Massachusetts Institute of Technology Department of Comparative Medicine and Committee of Animal Care. c-fos-tTA transgenic mice were generated as described in (*1*), by breeding TetTag mice (*2*) with C57BL/6J mice and selecting offspring carrying only the c-fos-tTA transgene. Mice had access to food and water *ad libitum* and were socially housed in numbers of two to five littermates until surgery. Following surgery, mice were singly housed. For behavioral experiments, all mice used for the experiments were male and 7–9 weeks old at the time of surgery and had been raised on food containing 40 mg kg^{-1} doxycycline (DOX) for at least one week before surgery, and remained on DOX food for the remainder of the experiments except for the target engram labeling days. For *ex vivo* electrophysiology experiments, mice were 24-28 days old at the time of surgery.

Engram labeling strategy

In order to label memory engram cells, we employed adeno-associated viruses that express either mCherry alone or ChR2 fused to an EYFP/mCherry fluorophore under the control of a tetracycline-responsive element (TRE)-containing promoter (AAV_9-TRE-mCherry, AAV_9-TRE-ChR2-EYFP, or AAV_9-TRE-ChR2-mCherry), which are active in cells that contain the tetracycline transactivator (tTA) (*1*). For each engram experiment, we injected one of these viruses into the target brain region of c-fos-tTA transgenic mice, which express tTA under the control of a *c-fos* promoter (fig. S1A) (*2*). Because *c-fos* is an activity-dependent gene, the c-fos-tTA transgene selectively expresses tTA in active cells (fig. S1B). Thus, active cells can express tTA that will then induce the virus to express mCherry or ChR2 in those cells. In order to restrict activity-dependent labeling to targeted training episodes the mice were fed DOX food, which sequesters tTA function and prevents virus expression. Subjects were then taken Off DOX one day prior to training in order to permit the labeling of memory engram cells (fig. S1C, D, E). Shining 473 nm blue light on a ChR2 positive neuron causes the opening of ChR2 channels, and the rapid influx of cations results in the depolarization of the neuron (*3*). Therefore, by shining blue light onto ChR2-labeled engram cells, memory recall can be directly evoked (*1*). Patch-clamp recordings *in vitro* confirmed that light successfully activated ChR2-labeled DG cells following contextual fear conditioning (CFC) (fig. S1F, G).

Virus-mediated gene expression

The recombinant AAV vectors used for viral production were pAAV-TRE-ChR2-EYFP described in (*1*), pAAV-TRE-ChR2-mCherry and pAAV-TRE-mCherry described in (*4*). The pAAV-hSyn1-HA-hM4Di-IRES-mCitrine plasmid was acquired from Bryan Roth at the University of North Carolina. The pAAV-CaMKIIα-ChR2-EYFP plasmid was acquired from Addgene. Plasmids were serotyped with AAV_8 or AAV_9 coat proteins and packaged at the University of Massachusetts Medical School Gene Therapy Center and Vector Core.
The recombinant AAV vectors were injected with viral titers of 1 X 10^{13} genome copy (GC) ml^{-1} for AAV_9-TRE-ChR2-EYFP, 8.0 × 10^{12} GC ml^{-1} for AAV_9-TRE-ChR2-mCherry, 1.4 X 10^{13} GC ml^{-1} for AAV_9-TRE- mCherry, 3.3 X 10^{12} GC ml^{-1} for AAV_9-hSyn1-HA-hM4Di-IRES-mCitrine, and 8.0 X 10^{12} GC ml^{-1} for AAV_8-CaMKIIα-ChR2-EYFP.

Stereotactic surgery procedure

Mice were anesthetized using 500 mg kg^{-1} avertin, or isoflurane. Bilateral craniotomies were performed using a 0.5 mm diameter drill and the viruses were injected using a glass micropipette attached to a 10 ml Hamilton microsyringe (701LT; Hamilton) through a microelectrode holder (MPH6S; WPI) filled with mineral oil. A microsyringe pump (UMP3; WPI) and its controller (Micro4; WPI) were used to maintain the speed of the injection at 60 nl min^{-1}. The needle was slowly lowered to the target site and remained for 5 min before beginning the injection. After the injection, the needle stayed for 10 minutes before it was slowly withdrawn. After withdrawing of

the needle, a custom implant containing two optic fibers (200 mm core diameter; Doric Lenses) was lowered above the injection site. Two jewelry screws were screwed into the skull on either side of bregma. A layer of adhesive cement (C&B Metabond) was applied followed with dental cement (Teets cold cure; A-M Systems) to secure the optic implant. A cap derived from the top part of an Eppendorf tube was inserted to protect the implant. Mice were given 1.5 mg kg^{-1} metacam as analgesic and remained on a heating pad until fully recovered from anesthesia. Mice were allowed to recover for at least 2 weeks before all subsequent behavioral experiments.

Ex vivo patch clamp recording

Stereotactic surgery

For AMPA/NMDA ratio experiments (Fig. 1A-E), entorhinal cortex (EC) injections of AAV_8-CaMKIIα-ChR2-EYFP (500 nl) were targeted unilaterally to (-4.7 mm anteroposterior (AP), +3.35 mm mediolateral (ML), - 3.3 mm dorsoventral (DV)), and dentate gyrus (DG) injections of AAV_9-TRE-mCherry (300 nl) were targeted unilaterally to (-2.0 mm AP, +1.3 mm ML, –1.9 mm DV).
For experiments involving spine counting (Fig. 1F, fig. S6, and fig. S7) and intrinsic physiological properties (fig. S4, fig. S6, and fig. S7), injections of AAV_9-TRE-ChR2-EYFP (300 nl) were targeted unilaterally to (-2.0 mm AP, +1.3 mm ML, –1.9 mm DV).
For fig. S4, DG injections of AAV_8-CaMKIIα-ChR2-EYFP (300 nl) were targeted unilaterally to (-2.0 mm AP, +1.3 mm ML, –1.9 mm DV).
For DG-CA3 connectivity experiments (Fig. 1G), DG injections of AAV_9-TRE-ChR2-EYFP (100 nl) were targeted unilaterally to (-2.0 mm AP, +1.3 mm ML, –1.9) mm DV, and CA3 injections of AAV_9-TRE-mCherry (150 nl) were targeted unilaterally to (-2.0 mm AP, +2.3 mm ML, –2.2 mm DV).

Animals and slice preparation

All *ex vivo* experiments were conducted blind to experimental group. Researcher 1 trained the animals and administered drug, while Researcher 2 dispatched the animals and conducted physiological experiments. Mice (P30-P40) were anesthetized with isoflurane, decapitated and brains were quickly removed. Sagittal slices (300 µm thick) were prepared in an oxygenated cutting solution at ~4°C by using a vibratome (VT1000S, Leica). Slices were then incubated at room temperature (~23°C) in oxygenated ACSF until the recordings. The cutting solution contained (in mM): 3 KCl, 0.5 $CaCl_2$, 10 $MgCl_2$, 25 $NaHCO_3$, 1.2 NaH_2PO_4, 10 D-glucose, 230 sucrose, saturated with 95%O_2 - 5%CO_2 (pH 7.3, osmolarity 340 mOsm). The ACSF contained (in mM): 124 NaCl, 3 KCl, 2 $CaCl_2$, 1.3 $MgSO_4$, 25 $NaHCO_3$, 1.2 NaH_2PO_4, 10 D-glucose, saturated with 95%O_2 - 5% CO_2 (pH 7.3, osmolarity 300 mOsm). Individual slices were transferred into a submerged experimental chamber and perfused with oxygenated ACSF warmed at 35°C (±0.5°C) at a rate of 3 ml/min during recordings.

Electrophysiology

Whole cell recordings in current clamp or voltage clamp mode were performed by using an IR-DIC microscope (BX51, Olympus) with a water immersion 40X objective (N.A. 0.8), equipped with four automatic manipulators (Luigs & Neumann) and a CCD camera (Orca R2, Hamamatsu Co). For all the recordings, borosilicate glass pipettes were fabricated (P97, Sutter Instrument) with resistances of 8 to 10 MΩ. For current clamp recordings, pipettes were filled with the following intracellular solution (in mM): 110 K-gluconate, 10 KCl, 10 HEPES, 4 ATP, 0.3 GTP, 10 phosphocreatine and 0.5% biocytin. The osmolarity of this intracellular solution was 290 mOsm and the pH was 7.25. The AMPA/NMDA ratio measurements were performed by adding 10 µM gabazine (Tocris) in the extracellular solution, and recordings in voltage clamp were performed by using the following intracellular solution (in mM): 117 cesium methansulfonate, 20 HEPES, 0.4 EGTA, 2.8 NaCl, 5 TEA-Cl, 4 Mg-ATP, 0.3 Na-GTP, 10 QX314, 0.1 spermine and 0.5% biocytin. The osmolarity of this intracellular solution was 290 mOsm and the pH was 7.3. Recordings were amplified using up to two dual channel amplifiers (Multiclamp 700B, Molecular Devices), filtered at 2 kHz, digitized (20 kHz), and acquired through an ADC/DAC data acquisition unit (ITC1600, Instrutech) by using custom made software running on Igor Pro (Wavemetrics). Access resistance (RA) was monitored throughout the duration of the experiment and data acquisition was suspended whenever the resting membrane

potential was depolarized above -50 mV or the RA was beyond 20 MΩ. All drugs used (Gabazine, NBQX, AP5, ANI) were provided by Tocris.

Optogenetics

Optogenetic stimulation was achieved through a 460 nm LED light source (XLED1, Lumen Dynamics) driven by TTL input with a delay onset of 25 µs (subtracted off-line for the estimation of latencies). Light power on the sample was 33 mW/mm^2. To test ChR2 expression, slices were stimulated with a single light pulse of 1 s, repeated 10 times every 5 s. To test synaptic connections, slices were stimulated with single light pulses of 2 ms, repeated 20 times every 5 s. In voltage clamp mode, cells were held at -70 mV, while in current clamp mode, response to optogenetic stimulation was measured at resting potential. DG-CA3 connectivity (Fig. 1G) was tested in current clamp mode, holding the cell at -70 mV. A train of 15 pulses at 20 Hz was delivered 20 times every 5 s and the average response was computed. The glutamatergic nature of the connection was confirmed by bath application of 10 µM NBQX (N = 4). The effect of ANI treatment on CA3 engram cells was evident from the measurement of the membrane capacitance (SAL: mCherry$^-$ 89.5 ± 7 pF, mCherry$^+$ 115 ± 9 pF, unpaired t test $P < 0.05$; ANI: mCherry$^-$ 103 ± 14 pF, mCherry$^+$ 95 ± 15 pF, unpaired t test $P = 0.7$).

Analysis

Synaptic connections, in voltage or current clamp mode, were determined by averaging 20 trials. EPSC amplitude was measured from the average maximum peak response by subtracting a baseline obtained 5 ms before light pulse starts (Fig. 1A-E). AMPA/NMDA ratios were measured in voltage clamp mode holding the voltage at -70 mV for AMPA current amplitude and holding the voltage at +40 mV for NMDA current amplitude measurement. The amplitude of the NMDA current was measured 100 ms after the onset of the light to avoid AMPA current overlap. The probability of DG-CA3 connectivity (Fig. 1G) was computed as, P = (successful tests/total test number). Error bars are approximated by binomial distribution. Spontaneous EPSCs (EPSCs) (fig. S2) were recorded at a holding potential of -70 mV in presence of Gabazine (10 µM). EPSCs were detected using an Igor Pro routine and were defined as inward currents with amplitudes exceeding two times the standard deviation of the baseline noise.
Granule cells expressing ChR2-EYFP, which in current clamp mode (at resting potential) responded to optogenetic stimulation with at least one action potential were considered engram cells and were selected for the analysis. The intrinsic electrophysiological properties (fig. S4) were measured in current clamp mode, holding the cell at –70 mV. Resting membrane potential was measured in current clamp mode without current injection. Action potential threshold was tested with a current ramp injection. Input resistance was measured by injecting a negative -120 pA current lasting 1 s. Membrane time constant was estimated through single exponential fit of the recovery-time from a –10 mV voltage deflection of 1 s duration. Excitability was estimated by linear fit of current (I) vs. firing rate (F) relationship.

Statistics

Statistical analysis was performed using Igor (Wavemetrics), MATLAB (Math works) or Excel (Microsoft). The distribution of the data was tested with the Kolmogorov-Smirnov test. A two sample Kolmogorov-Smirnov test, a Wilcoxon signed-rank test, a two-tailed paired or unpaired *t* test was employed for comparisons according to the application. Data are presented as mean ± SEM. To test significance of the connection probability, a Fisher's exact test was employed.

Post hoc immunocytochemistry

Recorded cells were filled with biocytin and subsequently recovered for morphological identification. Slices were first incubated with 4% PFA for 16 hr at 4°C. After washing with 0.5% Triton-X, slices were incubated in 5% normal goat serum (NGS) for 2 hr. Following NGS, slices were incubated in primary antibody (rabbit anti-RFP, 1:1000) overnight at 4°C. After washing with 0.5% Triton-X, slices were visualized by streptavidin CF633 (1:200, Biotium) and anti-rabbit Alexa-555. Before mounting, slices were incubated with DAPI (1:3000) for 30 min.

Spine density analysis

Experiments were conducted blind to experimental group. Researcher 1 imaged dendritic fragments, while Researcher 2 randomized images in advance of manual spine counting. Dentate granule cells were labeled with biocytin during patch clamp recordings. Fluorescence Z-stacks were taken by confocal microscopy (Zeiss LSM700), using 40 X objectives. Z-projected confocal images were generated by Zenblack (Zeiss). A total number of 16 granule cells were analyzed for spine examination (n = 4 cells per group x n = 4 groups). We analyzed 10 dendritic fragments of 10 µm length for each cell. To compute the spine density, the number of spines counted on each fragment was normalized by the cylindrical approximation of the surface of the specific fragment (Fig. 1F). The same applies for fig. S6, and fig. S7.

In vivo multi-unit electrophysiological recording

Using an anesthetized setup, multi-unit responses to optogenetic (ChR2) stimulation were recorded from c-fos-tTA mice injected with AAV_9-TRE-ChR2-EYFP virus in the DG. Mice were anesthetized by injection (10 ml kg^{-1}) of a mixture of ketamine (100 mg ml^{-1})/xylazine (20 mg ml^{-1}) and placed in the stereotactic system. Anesthesia was maintained by a series of booster doses of ketamine (100 mg kg^{-1}). An optrode consisting of a tungsten electrode (0.5 MΩ) attached to an optic fiber (200 µm core diameter), with the tip of the electrode extending beyond the tip of the fiber by 300 µm, was used for simultaneous optical stimulation and extracellular recording. The power intensity of light emitted from the optrode was calibrated to about 10 mW, which was consistent with the power intensity used in behavioral assays. To identify ChR2-positive cells, 15 ms light pulses at 0.2 Hz were delivered to the recording site every 50-70 µm. After light-responsive cells were detected, multi-unit activity in response to trains of 10 light pulses (15 ms) at 20 Hz was recorded. Activity was acquired using an Axon CNS Digidata 1440A system and analyzed using MATLAB, described in (*4*).

Behavior

Stereotactic injection and optic fiber implant

DG injections were targeted bilaterally to (-2.0 mm AP, +/- 1.3 mm ML, –1.9 mm DV). DG implants were placed at (-2.0 mm AP, +/- 1.3 mm ML, –1.9 mm DV). CA1 injections were targeted bilaterally to (-2.0 mm AP, +/- 1.5 mm ML, –1.5 mm DV). CA1 implants were placed at (-2.0 mm AP, +/- 1.5 mm ML, –1.4 mm DV). LA injections were targeted bilaterally to (-1.7 mm AP, +/- 3.45 mm ML, –4.2 mm DV). LA implants were placed at (-1.7 mm AP, +/- 3.45 mm ML, –4.0 mm DV). AAV_9-TRE-ChR2-EYFP volumes were 300 nl for DG and 500 nl for CA1. AAV_9-TRE-ChR2-mCherry volumes were 300 nl for DG and 200 nl for LA. AAV_9-hSyn1-HA-hM4Di-IRES-mCitrine volume was 500 nl for CA1. All injection sites were verified histologically. As criteria we only included mice with ChR2-EYFP or ChR2-mCherry expression limited to the targeted regions.

Optogenetics

For all DG and LA behavioral experiments, ChR2 was stimulated using a 473 nm laser delivering blue light at 20 Hz with a 15 ms pulse width, for the designated time period (*1*). For the CA1 experiment, 20 Hz proved ineffective (*4*), so here our stimulation protocol was adjusted to 4 Hz with a 15 ms pulse width.

Drug delivery

For consolidation experiments, 150 mg kg^{-1} anisomycin (ANI), or equivalent volume of saline (SAL), was delivered intra-peritoneally immediately after fear conditioning in the anteroom of the training context. For the ANI reconsolidation experiment, a second 150 mg kg^{-1} ANI dose was delivered 2 hours post-reactivation. For the cycloheximide (CHM) consolidation experiment 3 mg kg^{-1} CHM, or equivalent SAL, was delivered subcutaneously immediately after fear conditioning in the anteroom of the training context. For encoding experiments, 5 mg kg^{-1} clozapine-*N*-oxide (CNO) or SAL was delivered intra-peritoneally one hour before training, in the holding room.

Handling

All the behavioral experiments were conducted using mice that were 10 to 18 weeks of age, during the facility light cycle of the day (6.30 am to 6.30 pm). All behavioral subjects were individually habituated to handling by the investigator by handling for one minute on each of three separate days. Handling took place in the holding room where the mice were housed. Immediately prior to each handling session mice were transported by wheeled cart to and from the vicinity of the experimental context rooms, to habituate them to the journey.

Contextual Fear Conditioning – Consolidation (Figures 2A, 3B, 4A, S9, and S13)

Apparatus

For CFC experiments, two distinct contexts were employed, and used in different rooms. Context A chambers were 30 X 25 X 33 cm chambers with perspex floors, transparent square ceilings, red lighting, and scented with 0.25 % benzaldehyde. The ceilings of the Context A chambers were customized to hold a rotary joint (Doric Lenses) the exterior side of which was connected to a patch cord to a 473 nm laser that was controlled by a pulse generator. The interior side of the rotary joint was connected to two 0.32 M patch cords. All mice had patch cords fitted to the fiber implant prior to being placed in Context A. Two mice were run simultaneously in two identical Context A chambers. Context B chambers were 29 X 25 X 22 cm chambers with grid floors, opaque triangular ceilings, bright white lighting, and scented with 1 % acetic acid. Four mice were run simultaneously in four identical Context B chambers. All experimental groups were counter-balanced for chamber within contexts. All mice were conditioned in Context B, and tested in Contexts A and B. Experiments showed no generalization of conditioned response between contexts.

Floors of chambers were cleaned with Quatricide before and between runs. Mice were transported to and from the experimental room in their home cages using a wheeled cart. The cart and cages remained in an anteroom to the experimental rooms during all behavioral experiments.

Habituation

Four days prior to conditioning, all mice were habituated to Context A. Habituation sessions were 12 min in duration, consisting of four 3 min epochs, with the first and third epochs as the Light-Off epochs, and the second and fourth epochs as the Light-On epochs. During the Light-On epochs, the mouse received light stimulation (20 mW, 20 Hz, 15 ms) for the entire 3 min duration. At the end of 12 min, the mouse was immediately detached from the patch cords, returned to its home cage, and carted back to the holding room.

Training

Mice were trained in Context B using a CFC paradigm. Training sessions were 330 s in duration, and three 0.75 mA shocks of 2 s duration were delivered at 150 s, 210 s, and 270 s. SAL or ANI was delivered immediately after training. After fear conditioning, mice were placed in their home cages, and carted back to the holding room. Mice were kept on regular food without DOX for 24-30 hours prior to training. When training was complete, mice were switched back to food containing 40 mg kg^{-1} DOX.

Testing

All testing sessions in Context B were 180 s in duration. Testing conditions were identical to training conditioning, except that no shocks were presented. At the end of each session mice were placed in their home cages and carted back to the holding room.

All testing sessions in Context A were 12 min in duration, and were identical to the habituation sessions, consisting of four 3 min epochs, with the first and third epochs as the Light-Off epochs, and the second and fourth epochs as the Light-On epochs. During the Light-On epochs, the mouse received light stimulation (20 Hz for DG and LA, or 4 Hz for CA1) for the entire 3 min duration. At the end of 12 min, the mouse was immediately detached from the patch cords, returned to its home cage and carted back to the holding room.

Optogenetic Place Avoidance (OptoPA) - (Figure 3A)

Apparatus

Each OptoPA apparatus consisted of two distinct 15 × 15 × 20 cm zones (X and Y) connected to a triangular neutral zone as described in (*4*). Zone X consisted of black and white striped walls and contained a transparent floor with small irregular indentations. Zone Y consisted of black and white alternating dotted walls and contained a smooth plastic floor. The wall of the neutral zone was customized to hold a rotary joint (Doric Lenses) the exterior side of which was connected to a patch cord to a 473 nm laser that was controlled by a pulse generator. The interior side of the rotary joint was connected to two 0.5 M patch cords. All mice had patch cords fitted to the fiber implant prior to being placed in the apparatus. Two mice were run simultaneously in two identical OptoPA apparatuses.

Training contexts were 29 X 25 X 22 cm chambers with grid floors, opaque triangular ceilings, red lighting, and scented with 1 % acetic acid. Four mice were run simultaneously in four identical chambers. All experimental groups were counter-balanced for chamber within contexts.

Habituation

All mice were habituated to the OptoPA apparatus and laser stimulation procedure 4 days prior to training (taken from (*5*)). Mice were allowed to freely explore both zones X and Y during the 0–3 min baseline epoch, and the naturally preferred zone was determined as the target zone. During the 3–6 min and 9–12 min epochs (Light-On phases), light was administered only when a mouse was within the target zone. At the end of the 12 min, the mouse was immediately detached from the patch cords, returned to its home cage and carted back to the holding room.

Training

Mice were trained using a contextual fear-conditioning paradigm. Training sessions were 500 s in duration, and four 0.75 mA shocks of 2 s duration were delivered at 198 s, 278 s, 358 s and 438 s. SAL or ANI was delivered immediately after training. After fear conditioning, mice were placed in their home cages, and carted back to the holding room. To enable engram labeling, mice were kept on regular food without DOX for 24-30 hours prior to training. When training was complete, mice were switched back to food containing 40 mg kg^{-1} DOX.

Testing

All mice were subjected to 180 s test sessions in the training context, 1 day post training. At the end of each session mice were placed in their home cages and carted back to the holding room.

OptoPA tests were conducted 2 days post training. Mice were allowed to freely explore both zones X and Y during the 0–3 min baseline epoch, and the naturally preferred zone was determined as the target zone. During the 3–6 min and 9–12 min epochs (Light-On phases), light was administered only when a mouse was within the target zone. At the end of the 12 min, the mouse was immediately detached from the patch cords, returned to its home cage and carted back to the holding room. As criteria for inclusion in OptoPA experiments, during the baseline phases (0–3 min) of the OptoPA test day, mice that spent more than 90% of the time in one single zone were excluded. Additionally, mice that spent 100% of the time in one zone in any 3 min phase of the test were also excluded.

Analysis

Automated OptoPA tracking was done using Noldus EthoVision. Raw data was extracted and analyzed using Microsoft Excel. The difference scores (DS) reported in the main figures were obtained by subtracting the time spent in the target zone during the baseline phase from the average time spent in the target zone during the two on phases. Negative difference scores denote that the preference for the target zone during on phases is lower than the preference during the baseline phase.

Tone Fear Conditioning - (Figure 3C)

Apparatus

Three distinct contexts were employed and were used in different rooms. Context A chambers were 30 X 25 X 33 cm with perspex floors, a transparent square ceilings, red lighting, and scented with 0.25 % benzaldehyde. The ceilings of the Context A chambers were customized to hold a rotary joint (Doric Lenses) the exterior side of which was connected to a patch cord to a 473 nm laser that was controlled by a pulse generator. The interior side of the rotary joint was connected to two 0.32 M patch cords. All mice had patch cords fitted to the fiber implant prior to being placed in Context A. Context B chambers were 29 X 25 X 22 cm with grid floors, opaque triangular ceilings, bright white lighting, and scented with 1 % acetic acid. Context C chambers were 29 X 25 X 22 cm with glossy white plastic floors, no ceilings, dim lighting, and scented with 1 ml citral in a tray underneath.

Habituation

Habituation to Context A was identical to Contextual Fear Conditioning.

Training

Mice were trained in Context B using a tone fear conditioning paradigm. Training sessions were 420 s in duration, and three tone presentations (2 kHz and 75 dB) of 20 s duration were delivered at 180 s, 260 s, and 340 s and co-terminated with a 2 s 0.6 mA shock. SAL or ANI was delivered immediately after training. After fear conditioning, mice were placed in their home cages, and carted back to the holding room. To enable engram labeling, mice were kept on regular food without DOX for 24-30 hours prior to training. When training was complete, mice were switched back to food containing 40 mg kg^{-1} DOX.

Testing

All testing sessions in Context C were 420 s in duration and three tone presentations (2 kHz and 75 dB) of 20 s duration were delivered at 180 s, 260 s, and 340 s. Testing sessions in Context A were 12 min in duration, and were identical to the habituation sessions, consisting of four 3 min epochs, with the first and third epochs as the Light-Off epochs, and the second and fourth epochs as the Light-On epochs. During the Light-On epochs, the mouse received light stimulation for the entire 3 min duration. At the end of the 12 min, the mouse was immediately detached from the patch cords, returned to its home cage and carted back to the holding room.

Contextual Fear Conditioning – Reconsolidation Amnesia - (Figure 3D)

Apparatus, Habituation, and Training procedures used for the reconsolidation experiment were identical to those of the consolidation experiment (above). 1 day post training, contextual fear memory was reactivated by a 3 min re-exposure to the training Context B. SAL or ANI was delivered immediately after context re-exposure. 2 days post-training, amnesia due to disrupting reconsolidation was confirmed by 3 min test session in Context B. 3 days post-training, mice were subjected to a Context A test session consisting of four 3 min epochs, with the first and third epochs as the Light-Off epochs, and the second and fourth epochs as the Light-On epochs. During the Light-On epochs, the mouse received light stimulation (20 Hz) for the entire 3 min duration. At the end of the 12 min, the mouse was immediately detached from the patch cords, returned to its home cage and carted back to the holding room.

Inception of Fear Association - (Figure 3E)

Apparatus

Three distinct contexts were employed and were used in different rooms. Context A chambers were 29 X 25 X 22 cm with black cardboard floors, opaque triangular ceilings, red lighting, and scented with 1 % acetic acid. Context B chambers were 60 X 29 X 30 cm with white Perspex floors, white Perspex walls, no ceilings, bright white lighting, and unscented. The Context C chamber was 30 X 25 X 33 cm were with a metal grid floor, metallic square ceilings, dim white lighting, and scented with 0.25 % benzaldehyde. The ceiling of the Context C chamber was customized to hold a rotary joint (Doric Lenses) the exterior side of which was connected to a patch cord to a 473 nm laser that was controlled by a pulse generator. The interior side of the rotary joint was connected to two 0.32 M patch cords. Four mice were run simultaneously in four identical Context A chambers. Two mice were run simultaneously in two

identical Context B chambers. All experimental groups were counter-balanced for chamber within contexts. Mice were run individually in a single Context C chamber.

Context exposure

Mice were exposure to target Context A for 600 s. SAL or ANI was delivered immediately after context exposure. Immediately after context exposure, mice were placed in their home cages, and carted back to the holding room. To enable engram labeling, mice were kept on regular food without DOX for 24-30 hours prior to training. When training was complete, mice were switched back to food containing 40 mg kg^{-1} DOX.
1 day post-exposure to Context A, all mice were exposed to control Context B for 600 s while on DOX.

Fear Inception

2 days post-exposure to Context A, all mice were subjected to a fear inception procedure in Context C as described in (*4*). The inception session was 420 s in duration and consisted of 120 s of Light-Off, followed by 300 s of Light-On. Three 0.75 mA shocks of 2 s duration were delivered at 240 s, 300s, and 360 s. At the end of the 420 s, the mouse was immediately detached from the patch cords, returned to its home cage and carted back to the holding room.

Testing

Mice were tested in Context B 4 days post-exposure to Context A, and then tested to Context A 5 days post-exposure to Context A.

Quantification of freezing behavior

All behavioral experiments were analyzed blind to experimental group. Researcher 1 performed behavioral experiments and following the conclusion of each experiment all videos were randomized before manual scoring. Behavioral performance was recorded by digital video camera. For context and tone recall sessions, data were quantified using FreezeFrame software (ActiMetrics) with bout size set at 1.25 ms In the case of fear inception, freezing behavior was manually scored because the dark floor material resulted in inaccurate FreezeFrame data capture. Light stimulation during the habituation and test sessions interfered with the motion detection of the program, and therefore all light-induced freezing behavior was manually quantified by eye. Videos were scored individually, and investigators were blind to experimental condition and test day during all manual scoring.

Behavioral statistics

Data analysis and statistics were conducted using Prism (Graphpad software). Unpaired student's t-tests were used for independent group comparisons, with Welch's correction observed when group variances were significantly different. Paired student's t-tests were used to assess light-induced freezing behavior within groups.

Immunohistochemistry

Mice were dispatched by overdosing with 750–1000 mg kg^{-1} avertin and perfused transcardially with PBS, followed by 4 % paraformaldehyde (PFA) in PBS. Brains were extracted from the skulls and incubated in 4 % PFA at room temperature overnight. Brains were transferred to PBS and 50 µm coronal slices were taken using a vibratome and collected in PBS. For immunostaining, each slice was placed in PBS + 0.2 % Triton X-100 (PBS-T), with 5 % normal goat serum for 1 h and then incubated with primary antibody at $4^{o}C$ for 24 h. Slices then underwent three wash steps for 10 min each in PBS-T, followed by 1 h incubation with secondary antibody. Slices underwent three more wash steps of 10 min each in PBS-T, followed by mounting and cover-slipping on microscope slides. All imaging and analyses were performed blind to the experimental conditions. Antibodies used for staining were as follows: to stain for ChR2-EYFP, slices were incubated with primary chicken anti-GFP (Life Technologies) (1:1000) and visualized using anti-chicken Alexa-488 (Life Technologies) (1:200). For ChR2-mCherry, slices were stained using primary rabbit anti-RFP (Rockland) (1:1000) and secondary anti-rabbit Alexa-555 (Life Technologies)

(1:200). c-Fos was stained with rabbit anti-c-Fos (1:500, Calbiochem) and anti-rabbit Alexa-568 (Life Technologies) (1:500). Arc was stained with rabbit anti-Arc (1:300, Synaptic Systems) and anti-rabbit Alexa-568 (Life Technologies) (1:500).

Cell counting

All cell counting experiments were conducted blind to experimental group. Researcher 1 trained the animals and administered drug, while Researcher 2 dispatched the animals and conducted cell counting. To quantify the expression pattern of ChR2-EYFP and ChR2-mCherry in SAL and ANI injected c-fos-tTA mice, the number of EYFP/mCherry immunoreactive neurons were counted from 4-5 coronal slices per mouse (n = 3-5 for SAL and ANI groups, respectively). Coronal slices centered on coordinates covered by the optic fiber implants were taken from dorsal hippocampus (–1.82 mm to –2.30 mm AP). Fluorescence images were acquired using a Zeiss AxioImager.Z1/ApoTome microscope (20 X magnification). Automated cell counting analysis was performed using ImageJ software. The cell body layer of DG granule cells (upper blade), CA3 cells or sub-regions of the amygdala (BLA vs. CeA) were outlined as a region of interest (ROI) according to the DAPI signal in each slice. The number of EYFP-/mCherry-positive cells per section was calculated by thresholding EYFP/mCherry immunoreactivity above background levels. For statistical analysis, we used a one-way ANOVA followed by Tukey's multiple comparisons (α = 0.05). Data were analyzed using Microsoft Excel with the Statplus plug-in. All imaging and analyses were performed blind to the experimental conditions. Percentage engram cell reactivation data plotted in Fig. 3E calculated as (($cFos^+$, $ChR2^+$) / (Total $ChR2^+$)) X 100. Total engram cell reactivation was calculated as (($cFos^+$, $ChR2^+$) / (Total $DAPI^+$) X 100. $DAPI^+$ counts were approximation of 5 dorsal DG slices using ImageJ.

Stereotactic injection and optic fiber implant

DG injections of AAV_9-TRE-ChR2-EYFP were targeted bilaterally to (-1.9 mm AP, +/- 1.3 mm ML, –2.0 mm DV). DG implants were placed at (-1.9 mm AP, +/- 1.3 mm ML, –1.85 mm DV). CA3 injections of AAV_9-TRE-mCherry were targeted bilaterally to (-2.0 mm AP, +/- 2.0 mm ML, –1.9 mm DV). BLA injections of AAV_9-TRE-mCherry were targeted bilaterally to (-1.4 mm AP, +/- 3.1 mm ML, –4.6 mm DV). All virus volumes were 300 nl. As criteria we only included mice with ChR2-EYFP expression limited to the targeted region.

Amygdala activation in amnesia - (Figure 4A-C)

Four groups of c-fos-tTA mic e injected with AAV_9-TRE-ChR2-EYFP in the DG along with optic fiber implants were used for this experiment. Memory engram cells for contextual fear conditioning (CFC) were labeled in the DG of all groups. A day after training, two groups of mice (Saline Natural Cues, Anisomycin Natural Cues) were returned to the conditioning context (Context B) for a natural memory recall test followed by timed perfusions; performed to identify recall-induced $cFos^+$ cells. The remaining groups (Saline ChR2, Anisomycin ChR2) were placed in Context A for DG engram activation followed by timed perfusions. By this protocol, we quantified $cFos^+$ neurons in the amygdala (CeA, BLA) following either natural recall or DG engram activation.

Cellular connectivity in amnesia - (Figure 4D-K)

In support of the physiological connectivity data in Figure 1G, four groups of c-fos-tTA mice injected with AAV_9-TRE-ChR2-EYFP in the DG and AAV_9-TRE-mCherry in CA3 and BLA along with optic fiber implants were prepared for this experiment. Memory engram cells for CFC were labeled in DG, CA3 and BLA of all groups. A day after training, two groups of mice (Saline Natural Cues, Anisomycin Natural Cues) were returned to the conditioning context (Context B) for a natural memory recall test followed by timed perfusions. The remaining groups (Saline ChR2, Anisomycin ChR2) were placed in Context A for DG engram activation followed by timed perfusions. This procedure allowed us to quantify the percentage of engram neurons in CA3 and BLA that were re-activated ($cFos^+$) by either natural recall or DG engram activation.

Supplementary Figures

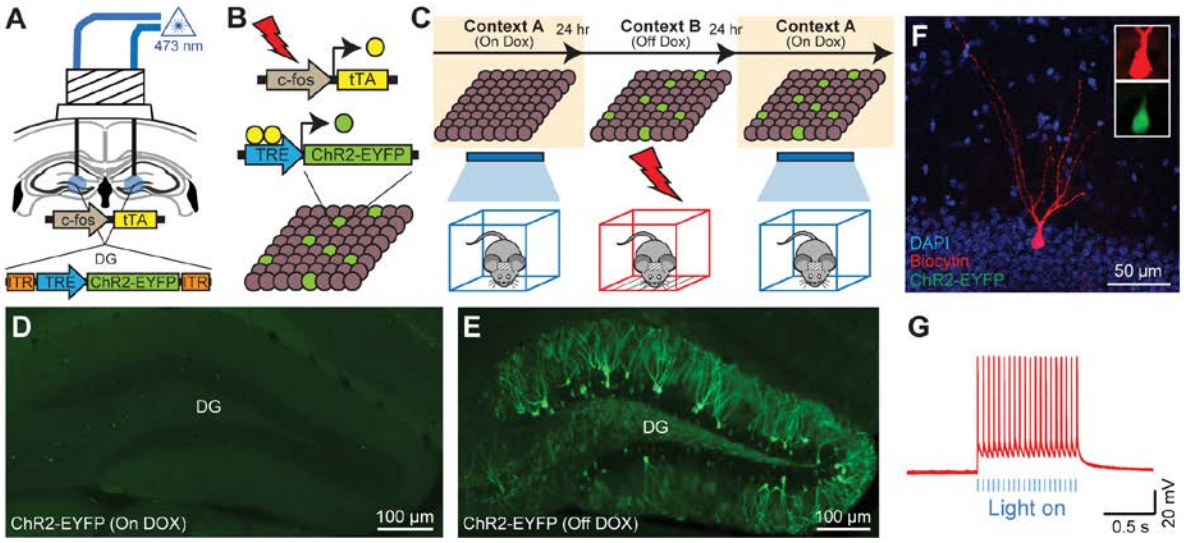

Figure S1: Labeling Dentate Gyrus Engram Cells with ChR2.

(A) Adeno-associated virus carrying *ChR2* gene under the control of a TRE promoter (AAV_9-TRE-ChR2-EYFP) was stereotactically injected in the dentate gyrus (DG) of c-fos-tTA transgenic mice. Following virus injections, bilateral optic fibers were implanted into the DG.

(B) When the *c-fos* promoter is active, tTA is expressed in cells. tTA protein binds to the TRE promoter, resulting in the expression of ChR2-EYFP. DOX prevents binding of tTA to the TRE promoter, restricting expression of ChR2 to defined temporal windows.

(C) Naïve, unlabeled mice were habituated to the patch cord and laser in Context A while On DOX. Mice were taken Off DOX 24-30 hours prior to CFC in Context B. Mice were placed back On DOX immediately after training. DG engrams were evoked by blue laser stimulation of the DG in Context A, at least 24 hours after training.

(D) Representative image showing a DG section from a c-fos-tTA mouse injected with AAV_9-TRE-ChR2-EYFP that was kept On DOX during training. No significant expression of ChR2-EYFP was observed, demonstrating DOX control over the labeling method.

(E) Representative image showing a DG section from a c-fos-tTA mouse injected with AAV_9-TRE-ChR2-EYFP, Off DOX from 24 hours before training. Sparse ChR2-EYFP expression occurs across the DG.

(F) Representative image of a ChR2-EYFP labeled DG neuron injected with biocytin during patch clamp recording.

(G) Blue light stimulation (20 pulses, 20 Hz, 15 ms each) of ChR2-EYFP labeled DG neuron resulted in spikes.

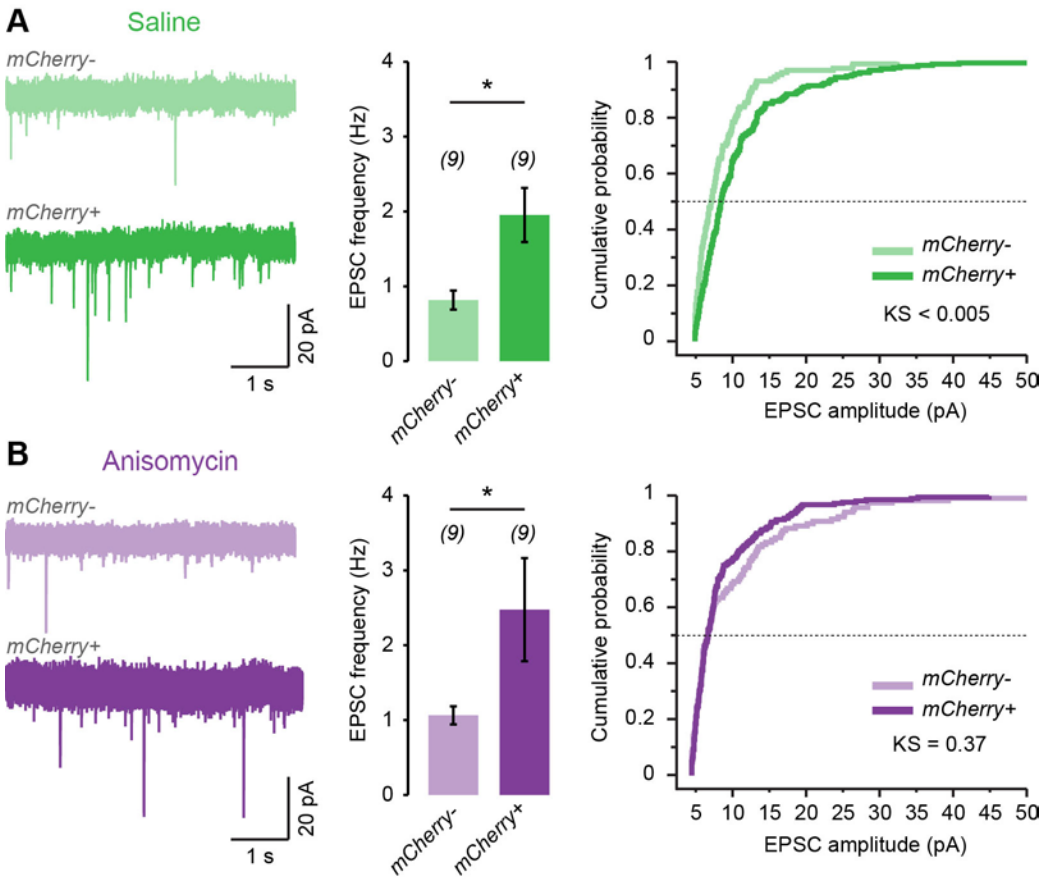

Figure S2: Analysis of Spontaneous EPSCs.

(A) Example of spontaneous EPSC recordings from mCherry$^-$ and mCherry$^+$ DG granule cells collected from cfos-tTA mice injected with AAV$_9$-TRE-mCherry in DG (same cells of Fig. 1A-E). Mice were injected with saline immediately after CFC and sacrificed 24 hr later for *ex vivo* recording. The mCherry$^+$ group displays higher EPSC frequency (two tailed paired t-test, $P < 0.05$) and higher EPSC amplitude than the mCherry$^-$ group (Kolmogorov-Smirnov test, $P < 0.005$).

(B) Example of spontaneous EPSC recordings from mCherry$^-$ and mCherry$^+$ DG granule cells collected from cFos-tTa mice injected either with AAV$_9$-TRE-mCherry in the DG. Mice were injected with anisomycin immediately after CFC and sacrificed 24 hr later for *ex vivo* recording. The mCherry$^+$ group displays higher EPSC frequency than the mCherry$^-$ group (two tailed paired t-test, $P < 0.05$) but the distributions of EPSC amplitudes are similar (Kolmogorov-Smirnov test, $P = 0.37$).

The mCherry$^+$ cells of the saline group display higher EPSC amplitudes than the mCherry$^+$ cells of the anisomycin group (Kolmogorov-Smirnov test, $P < 0.001$), whereas the mCherry$^-$ cells of the saline and the anisomycin group display similar EPSC amplitudes (Kolmogorov-Smirnov test, $P = 0.12$).

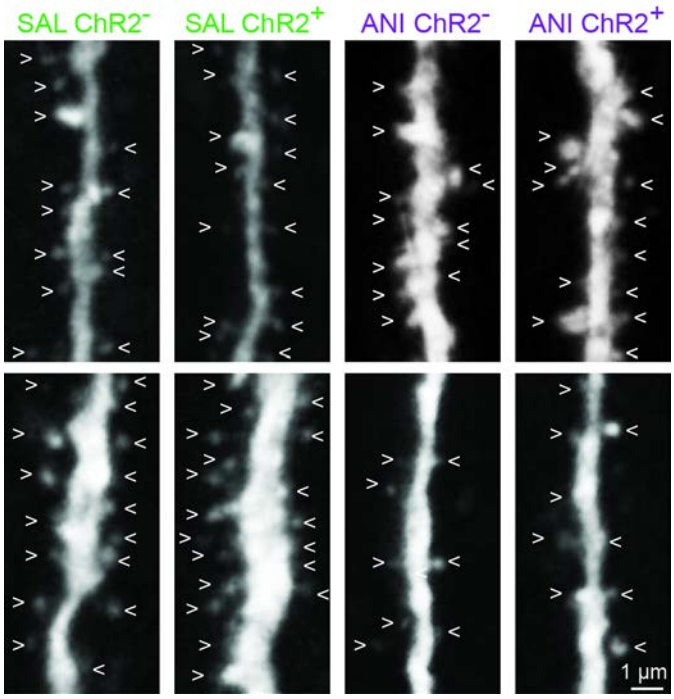

Figure S3: Confocal images of dendritic spines.

Two series (top and bottom) of confocal images of dendritic spines form $ChR2^+$ and $ChR2^-$ DG granule cell dendrites from the Saline (SAL) or the Anisomycin (ANI) group. Scale bar is the same for all the images.

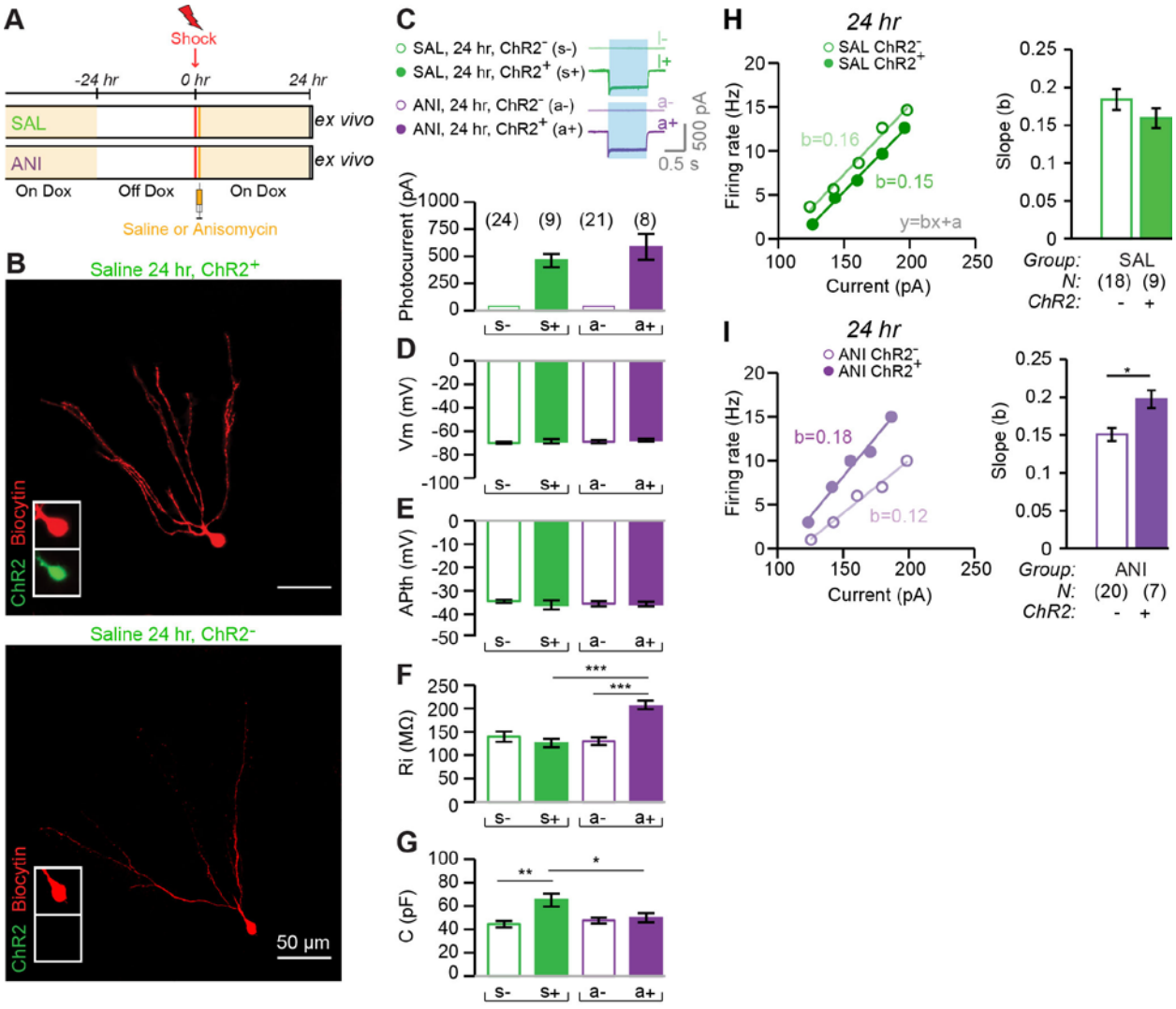

Figure S4: Physiological Profiling of DG Engram Cells.

(A) Schematic of *ex vivo* physiological experiments. c-fos-tTA mice with AAV_9-TRE-ChR2-EYFP injected into the DG were taken Off DOX 24 hrs before CFC, administered either SAL or ANI, and dispatched 24 hrs post-training,

(B) Representative images of $ChR2^+$ and $ChR2^-$ DG cells taken from the SAL group.

(C-I) Intrinsic physiological properties of engram ($ChR2^+$) and non-engram ($ChR2^-$) cells of the SAL (green), and ANI (purple) groups.

(C) Photocurrent measurements (pA) for $ChR2^+$ and $ChR2^-$ cells. Traces are displayed above bar charts. Blue light evoked comparable current influx in $ChR2^+$ cells but not in $ChR2^-$ cells of all three groups. Cell numbers in parentheses.

(D) Resting membrane potential measurements (Vm) for $ChR2^+$ and $ChR2^-$ cells across groups

(E) Action potential threshold (APth) for $ChR2^+$ and $ChR2^-$ cells across groups.

(F) Input resistance (Ri) for $ChR2^+$ and $ChR2^-$ cells across groups.

(G) Membrane capacitance (C) for $ChR2^+$ and $ChR2^-$ cells across groups.

(H, I) Examples of relationship between current injection and firing rate for the SAL (H) and ANI (I) groups, for engram $ChR2^+$ and non-engram $ChR2^-$ cells. Data are approximated by linear fit (gray formula in H) and the average value of the slope (b) is displayed in the bar charts. The $ChR2^+$ cells from the SAL group (H) display an excitability level similar to $ChR2^-$ cells. The $ChR2^+$ cells from the ANI group (I) display a significant 31% increase in excitability compared to $ChR2^-$ cells.

Data are represented as mean ± SEM. Statistical comparison are performed by using unpaired t tests, * $p < 0.05$, ** $p < 0.05$, and *** $p < 0.001$.

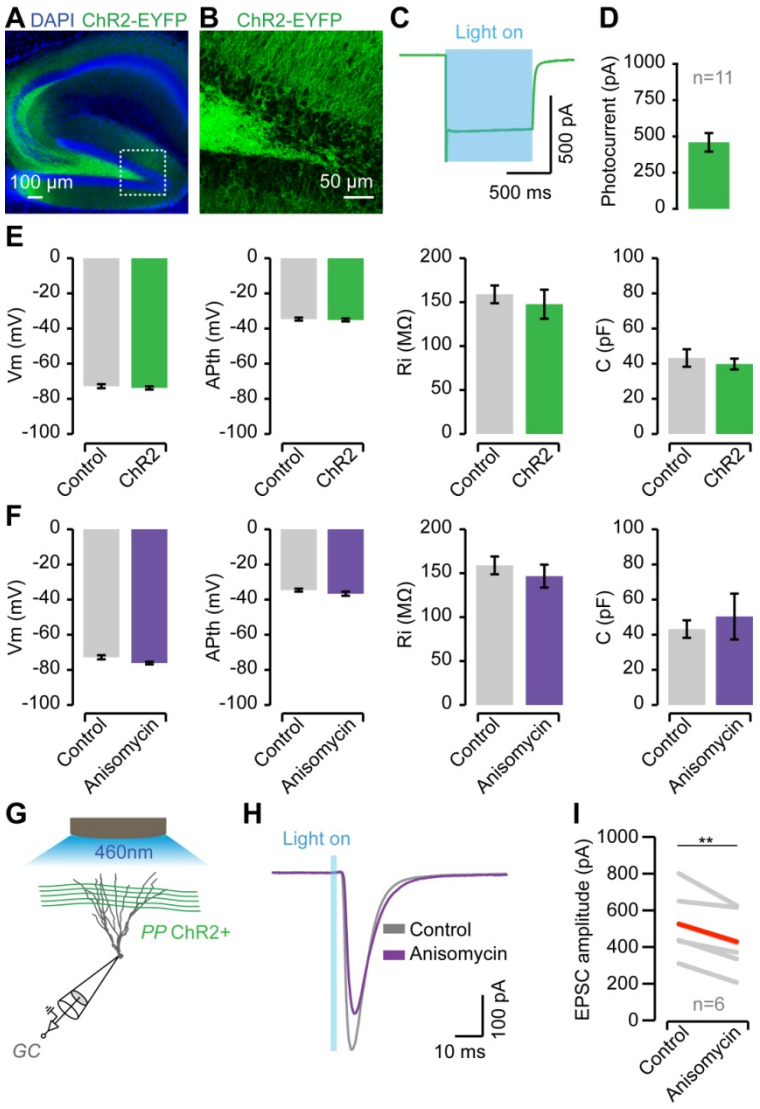

Figure S5: ChR2 and ANI have no Effect on the Intrinsic Properties of DG Granule Cells.

(A-B) The DG of c-fos-tTA transgenic mice were infected using an AAV_8-CaMKIIα-ChR2-EYFP virus. B, from the dotted-line box in A).

(C-D) Optogenetic stimulation of DG cells during voltage clamp recording revealed a robust photocurrent comparable to what was previously shown in fig. S4C.

(E) ChR2 expression had no effect on the intrinsic properties (resting membrane potential Vm, action potential threshold APth, input resistance Ri and capacitance C) of DG cells ($ChR2^+$ cells n = 11, $ChR2^-$ cells n = 16).

(F) Direct bath application of 40 µM ANI had no effect on the intrinsic properties of DG cells (control n = 11, ANI n = 14).

(G) Voltage clamp recording of a DG cell combined with optogenetic stimulation of $ChR2^+$ axons of the perforant path.

(H) Examples of excitatory postsynaptic currents (EPSCs) recorded in DG cells responding to optogenetic stimulation of the $ChR2^+$ axons of the perforant path in control conditions and following ANI bath application. Note the mild difference.

(I) Average EPSCs of experiments described in panel G-H ($n = 6$, paired t test ** $p < 0.01$).

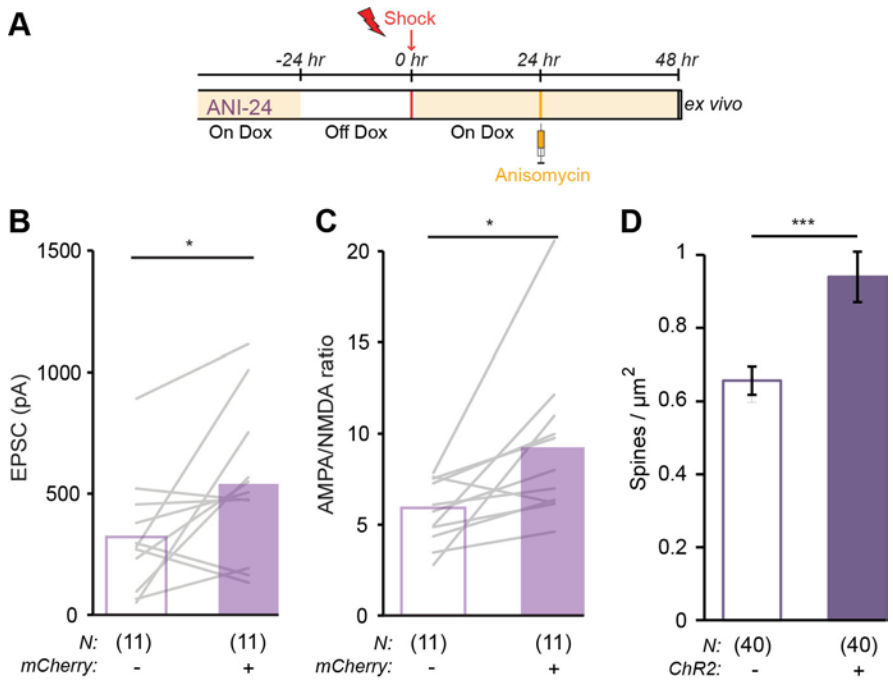

Figure S6: Anisomycin Injection Outside of the Memory Consolidation Window does not Affect Synaptic Strength, AMPA/NMDA Receptor Current Ratio, or Dendritic Spine Density.

(A) cfos-tTA mice injected in the DG either with AAV_9-TRE-mCherry (for synaptic analysis) or AAV_9-TRE-ChR2-EYFP (for spine density analysis) were taken off DOX 24 hr before exposure to contextual fear conditioning, injected with anisomycin 24 hr later and then sacrificed 24 hr after injection for *ex vivo* recording.

(B) Analysis of synaptic strength. The $mCherry^+$ group displays higher synaptic strength than the $mCherry^-$ group (two tailed paired t-test, $P < 0.05$).

(C) Analysis of AMPA/NMDA receptors ratio. The $mCherry^+$ group displays higher AMPA/NMDA receptors ratio than the $mCherry^-$ group (two tailed paired t-test, $P < 0.05$).

(D) Dendritic spine density analysis of $ChR2^+$ and $ChR2^-$ DG granule cells. The $ChR2^+$ group displays higher spine density than the $ChR2^-$ group (two tailed unpaired t-test, $P < 0.001$).

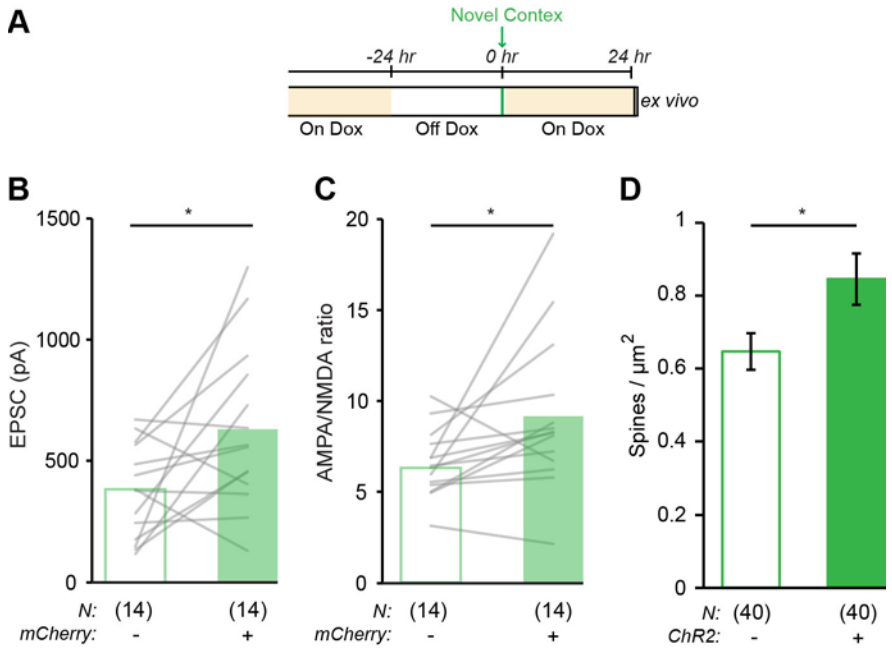

Figure S7: Effect of Exposure to Novel Context on Synaptic Strength, AMPA/NMDA Receptors Current Ratio, and Dendritic Spine Density.

(A) cfos-tTA mice injected in DG either with AAV_9-TRE-mCherry (for synaptic analysis) or AAV_9-TRE-ChR2-EYFP (for spine density analysis) were taken off DOX 24 hr before a 5 min. exposure to a novel context and then sacrificed 24 hr later for ex vivo recording.

(B) Analysis of synaptic strength. The $mCherry^+$ group displays higher synaptic strength than the $mCherry^-$ group (two tailed paired t-test, $P < 0.05$).

(C) Analysis of AMPA/NMDA receptors ratio. The $mCherry^+$ group displays higher AMPA/NMDA receptors ratio than the $mCherry^-$ group (two tailed paired t-test, $P < 0.05$).

(D) Dendritic spine density analysis of $ChR2^+$ and $ChR2^-$ DG granule cells. The $ChR2^+$ group displays higher spine density than the $ChR2^-$ group (two tailed unpaired t-test, $P < 0.05$).

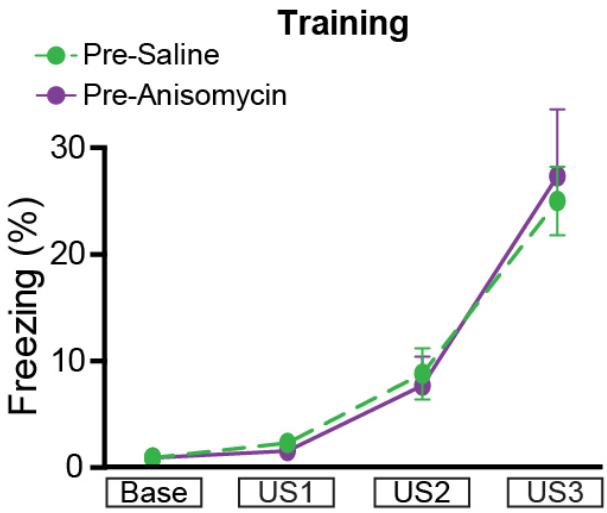

Figure S8: Response to Shock During CFC.

For the DG consolidation experiment (Fig. 2), naïve implanted c-fos-tTA mice were subjected to a CFC protocol while Off DOX, where three 0.75 mA shocks (unconditioned stimulus US1-3) of 2 s duration were delivered at 150 s, 210 s, and 270 s. No difference in unconditioned freezing behavior was observed between the two groups.

Data presented as mean ± SEM.

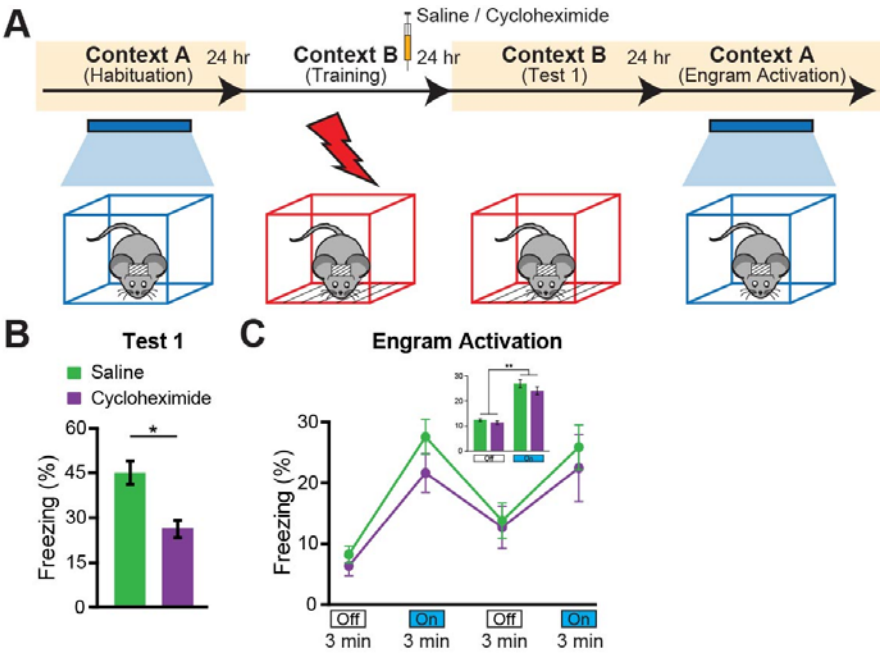

Figure S9: Optogenetic Stimulation of DG Engram Cells Retrieves fear memory in CHM-Induced Retrograde Amnesia.

(A) Schematic of the behavioral schedule used for experiments.

(B) Long-term memory recall in Context B, 1 day post-training. CHM group (N = 9) displayed significantly less freezing behavior to natural contextual cues than the SAL group (N = 9), ($p < 0.04$).

(C) Light-induced memory recall in Context A, 2 days post-training with Light-Off and Light-On epochs. Freezing levels for the two Light-Off and Light-On epochs are further averaged in the inset. Significant freezing due to light stimulation was observed in both the SAL ($p < 0.001$) and CHM groups ($p < 0.01$). Light-induced freezing levels did not differ between groups.

Data presented as mean ± SEM.

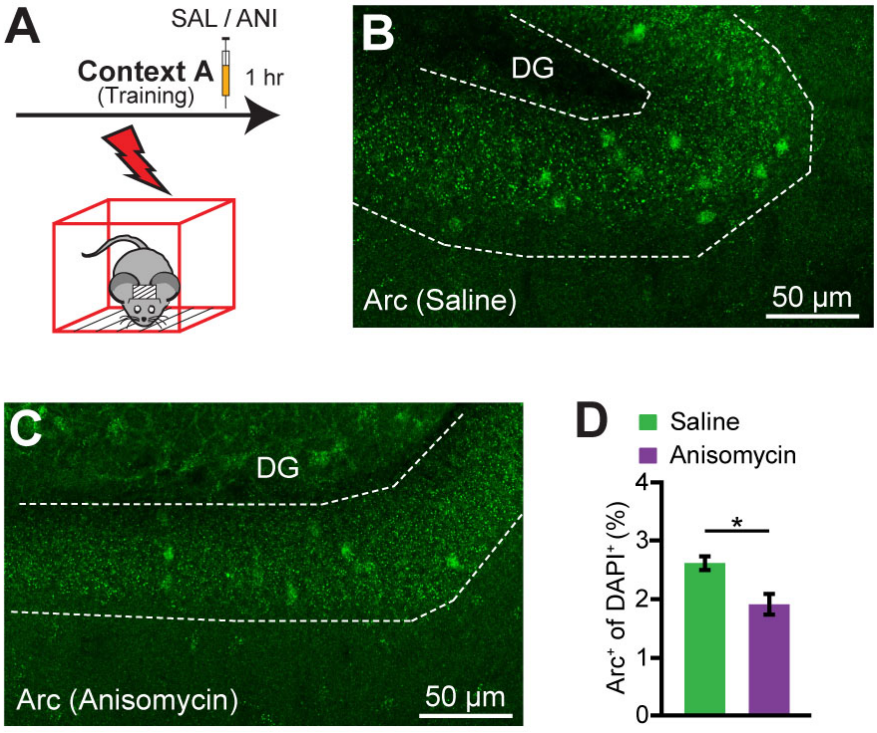

Figure S10: Post-Training Anisomycin Impairs DG Protein Synthesis.

(A) Schematic of the behavioral schedule used for experiments. Mice were pefused 1 hour post-training.

(B) Representative image of Arc staining in the DG of mice treated with saline.

(C) Representative image of Arc staining in the DG of mice treated with anisomycin.

(D) Average percentages of Arc^+ DG cells of SAL and ANI groups.

Data presented as mean ± SEM, * $p < 0.05$.

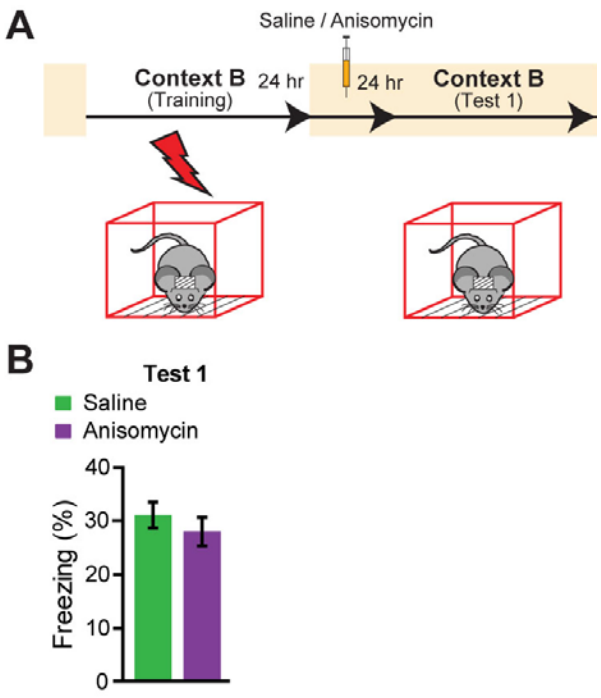

Figure S11: Anisomycin Delivery 24 hours Post-Training did not Induce Retrograde Amnesia.

(A) Schematic of the behavioral schedule used for experiments.

(B) Long-term memory recall in Context B, 1 day post-drug treatment. ANI group (N = 11) displayed equivalent freezing behavior to SAL group (N = 11).

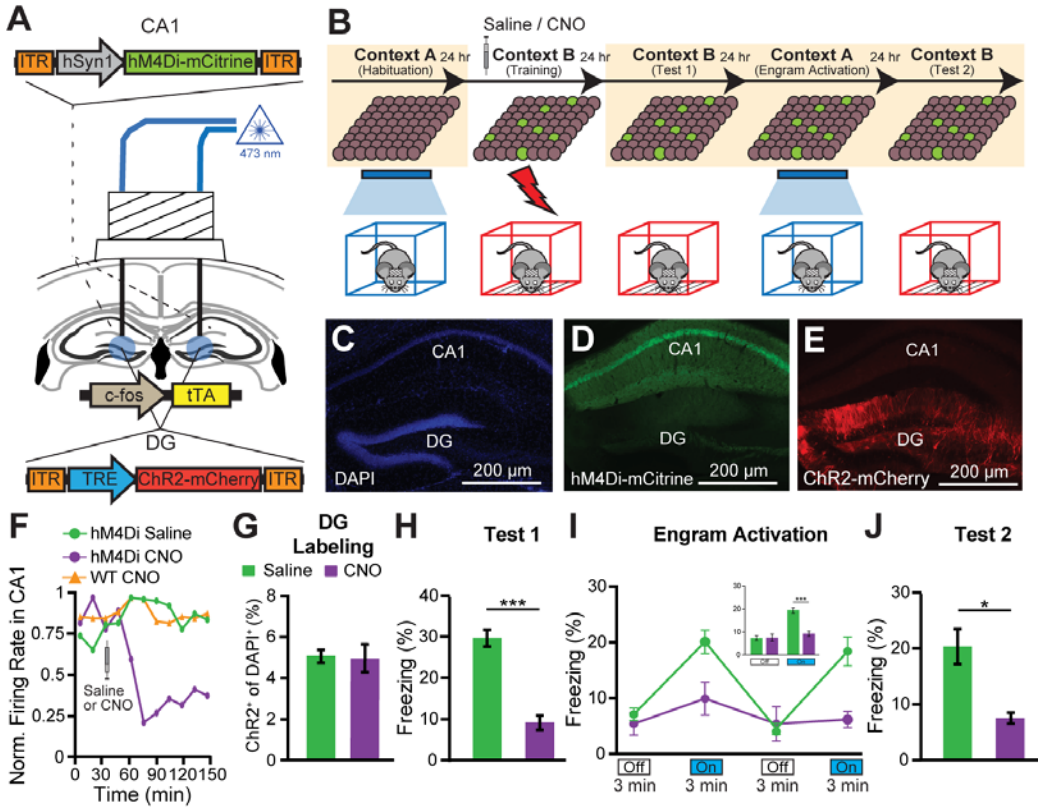

Figure S12: Optogenetic Stimulation of Engram Cells Does Not Retrieve Fear Memory following Anterograde Amnesia due to Impaired Encoding.

(A) An AAV virus carrying the inhibitory DREADDs hM4Di receptor under the control of a hSyn1 promoter (AAV_9-hSyn1-hM4Di-mCitrine) was stereotactically injected in CA1 of c-fos-tTA transgenic mice, with AAV_9-TRE-ChR2-mCherry injected into the DG. Following virus injections, bilateral optic fibers were implanted into DG.

(B) Schematic of the behavioral schedule used for memory encoding experiment. Depictions of DG cell populations. Mice were taken off 24-30 hrs before contextual fear conditioning in Context B and SAL or CNO (5 mg kg^{-1}) 1 hr before training.

(C-E) Representative images showing a hippocampal section from a c-fos-tTA mouse expressing hM4Di-mCitrine in CA1, and ChR2-mCherry in DG.

(F) CNO administration triggered hM4Di receptors to inhibit CA1 neuronal firing.

(G) $ChR2^+$ cell counts from DG sections of SAL (n = 4) and CNO (n = 4) treated c-fos-tTA mice. CNO treatment did not impair ChR2 labeling of DG engram cells.

(H) Long-term memory recall in Context B, 1 day post-training. The CNO group (N = 13) showed significantly less freezing behavior than the SAL group (N = 11), ($p < 0.001$).

(I) Light-induced memory recall in Context A, 2 days post-training with Light-Off and Light-On epochs. Freezing levels for the two Light-Off and Light-On epochs are further averaged in the inset. Significant freezing due to light stimulation was observed in both the SAL ($p < 0.0001$) and CNO groups ($p < 0.05$). Light-induced freezing was significantly lower in the CNO group (18.2% ± 1.3% versus 9.3% ± 1.6% freezing; $p < 0.0005$).

(J) Long-term memory recall in Context B, 3 days post-training. The CNO group showed significantly less freezing behavior than the SAL group (20.7% ± 4.7% versus 8.9% ± 1.7% freezing; $p < 0.05$).

Data presented as mean ± SEM.

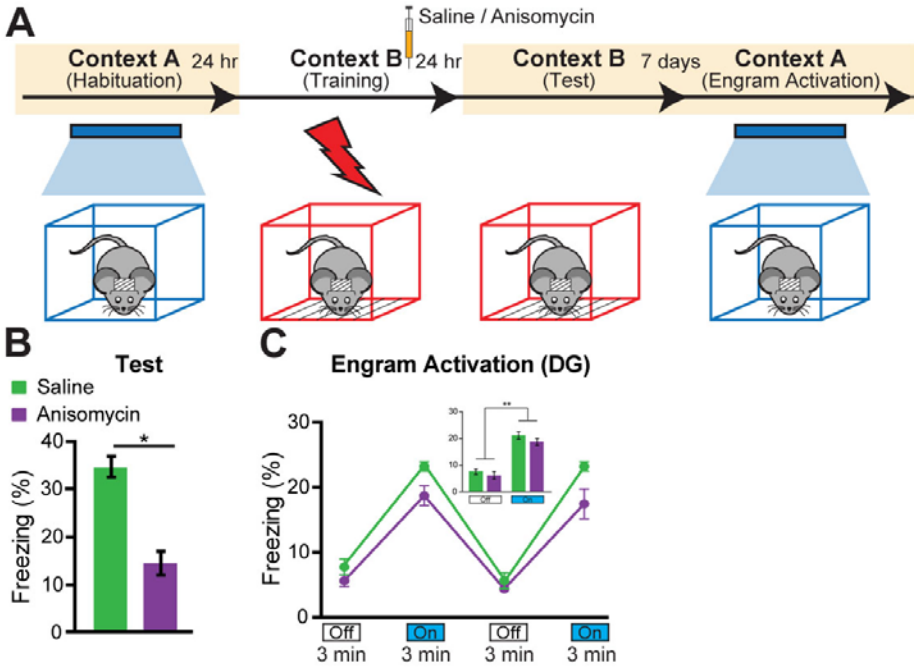

Figure S13: Optogenetic Stimulation of DG Engram Cells Retrieves Fear Memory 8 Days After Impaired Consolidation

(A) Schematic of the behavioral schedule used for experiments.

(B) Long-term memory recall in Context B, 1 day post-training. ANI group (N = 8) displayed less freezing behavior to natural contextual cues than the SAL group (N = 7, $p = 0.015$).

(C) Light-induced memory recall in Context A, 8 days post-training with Light-Off and Light-On epochs. Freezing levels for the two Light-Off and Light-On epochs are further averaged in the inset. Significant freezing due to light stimulation was observed in both the SAL ($p < 0.005$) and ANI groups ($p < 0.005$). Light-induced freezing levels did not differ between groups.

Data presented as mean ± SEM.

References

1. X. Liu *et al.*, *Nature* **484**, 381 (Apr 19, 2012).
2. L. G. Reijmers, B. L. Perkins, N. Matsuo, M. Mayford, *Science* **317**, 1230 (Aug 31, 2007).
3. E. S. Boyden, F. Zhang, E. Bamberg, G. Nagel, K. Deisseroth, *Nat Neurosci* **8**, 1263 (Sep, 2005).
4. S. Ramirez *et al.*, *Science* **341**, 387 (Jul 26, 2013).
5. R. L. Redondo *et al.*, *Nature* **513**, 426 (Sep 18, 2014).